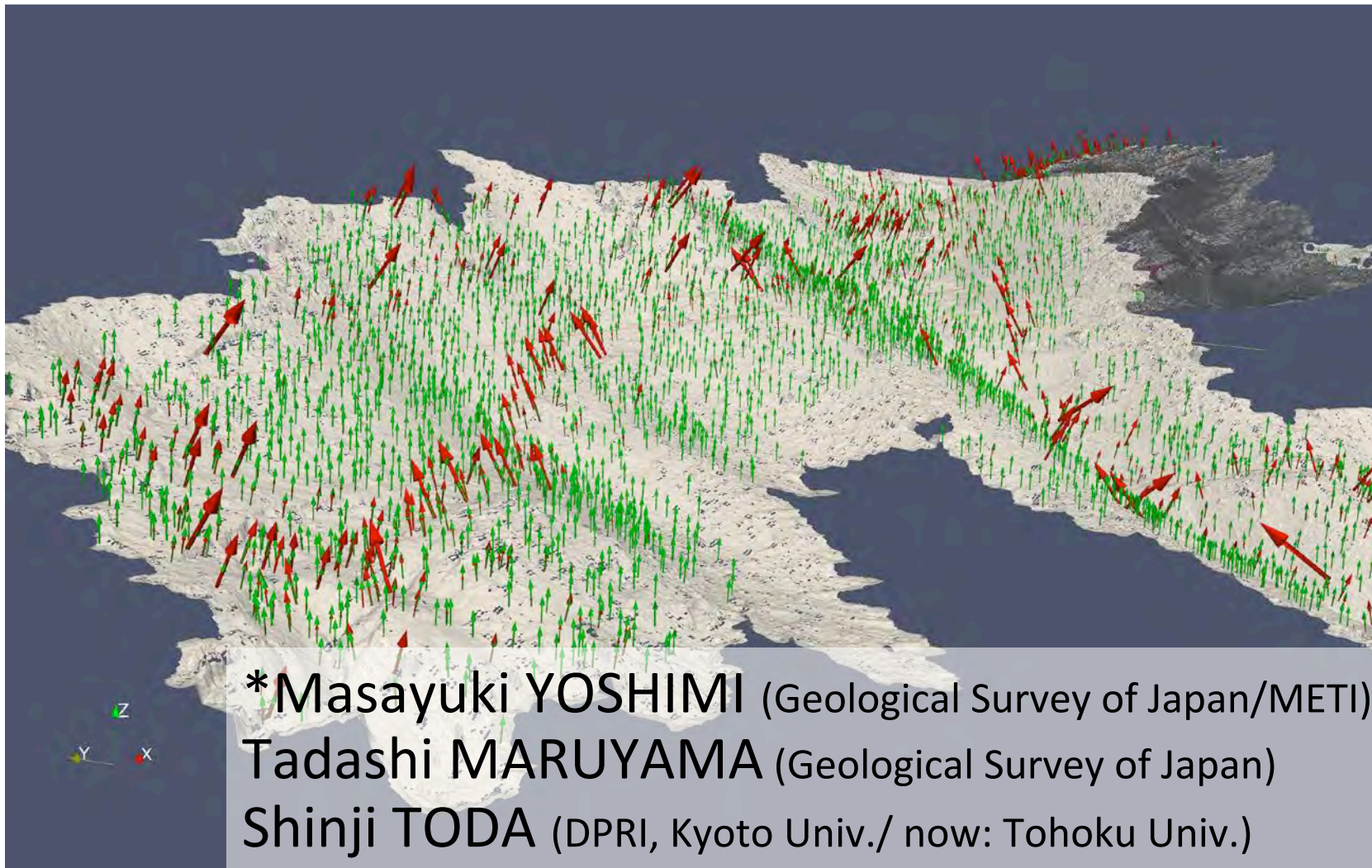
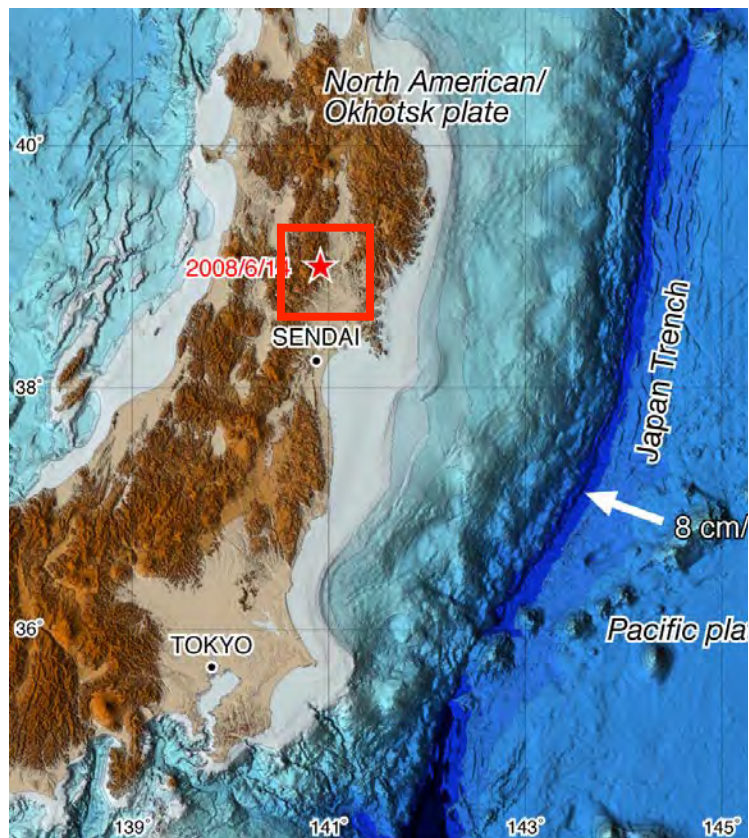


Superfine mapping of the earthquake surface ruptures in the forests with terrestrial LiDAR

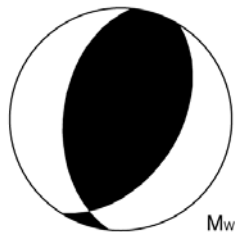
18 Sep. 2013 VISES workshop@ERI



2008 Iwate-Miyagi Inland earthquake (M6.9)



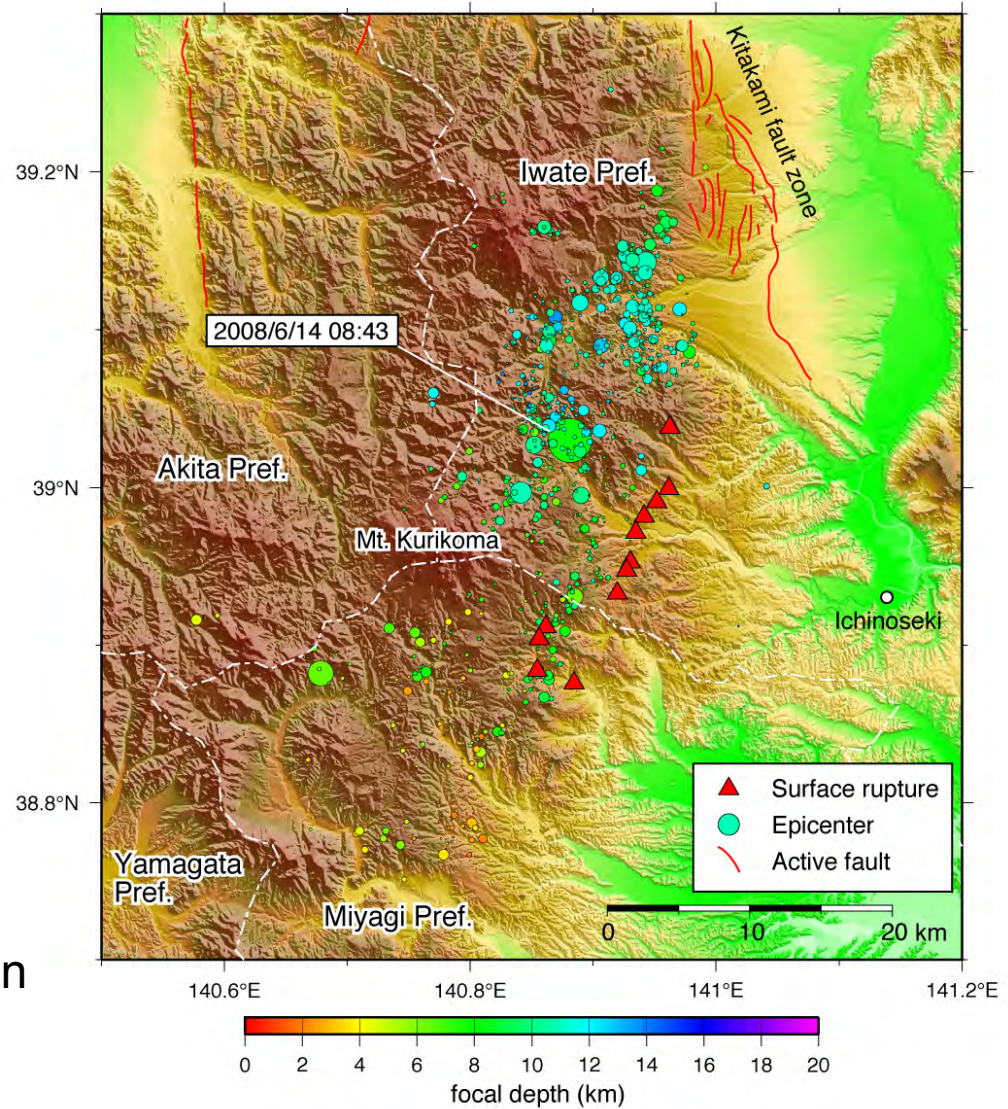
Focal mechanism (NIEC)
Mainshock



WNW-ESE compression

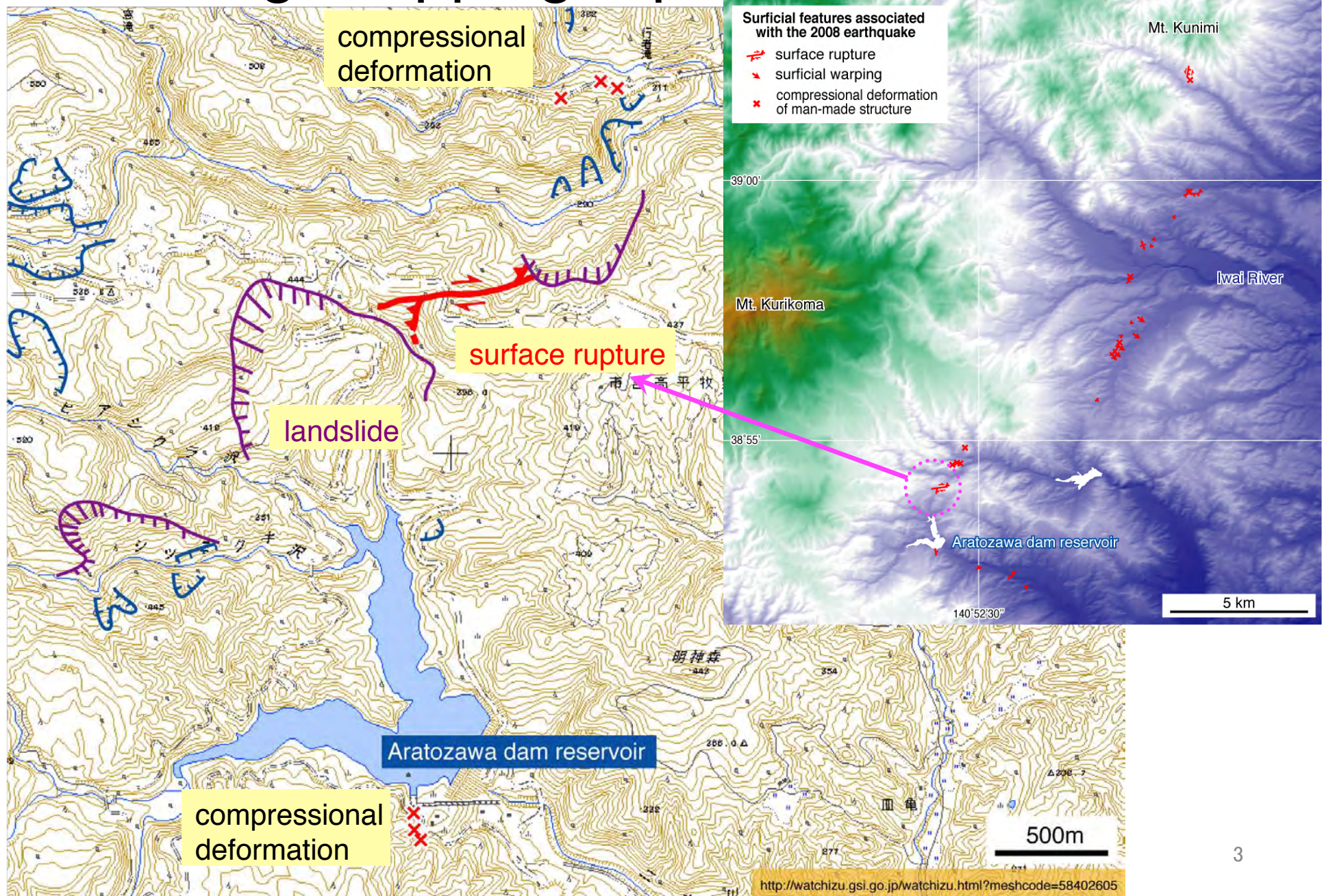
Mw 6.9
<http://www.f>

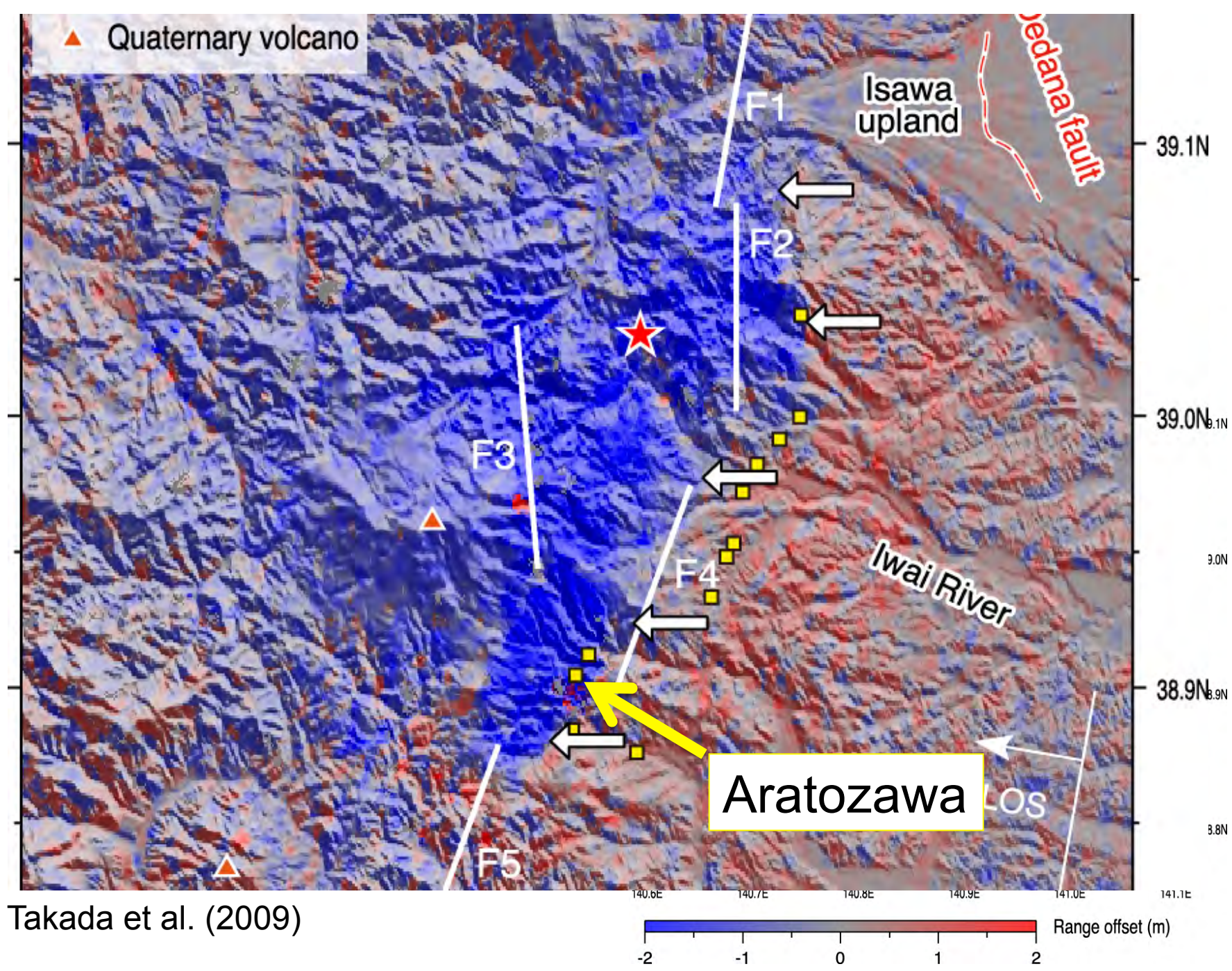
Toda et al. (2010)



We found spotty surface ruptures along east margin of the source area

Large slipping rupture at the south



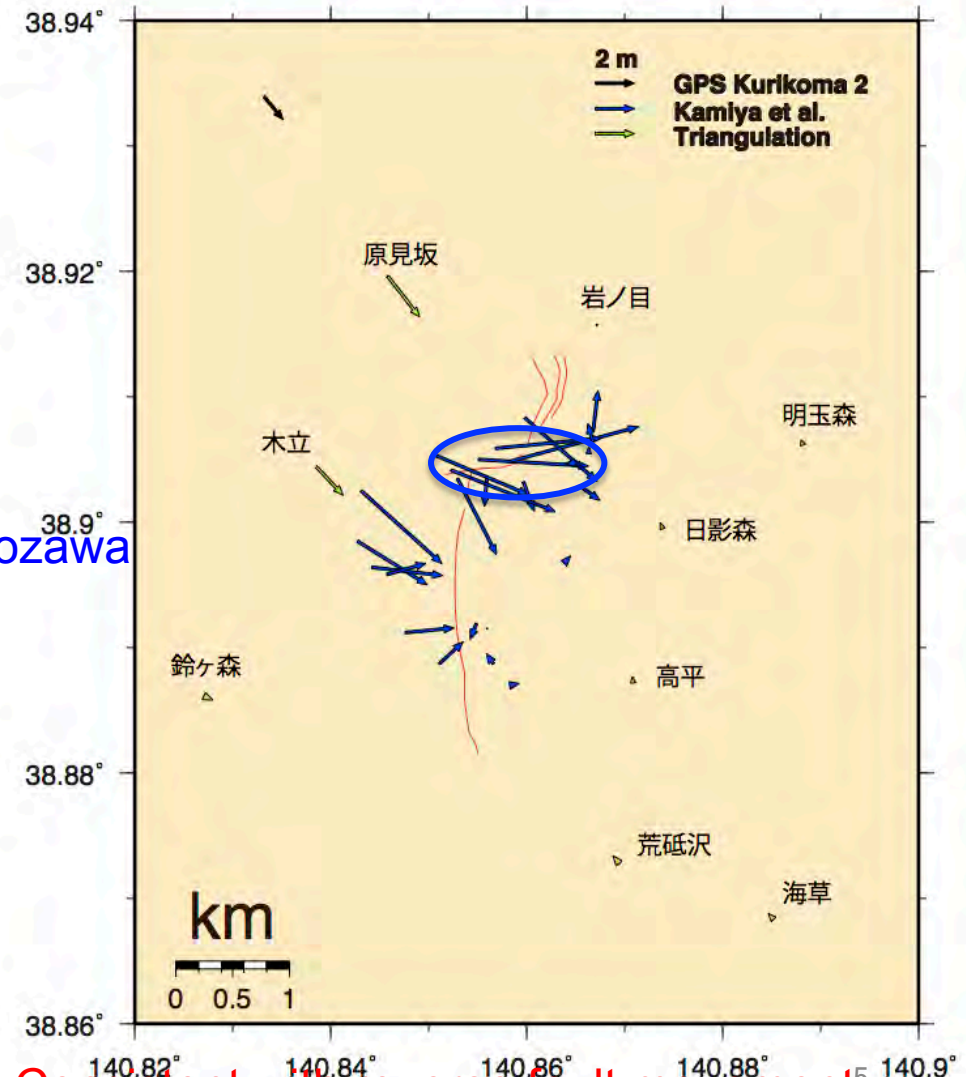
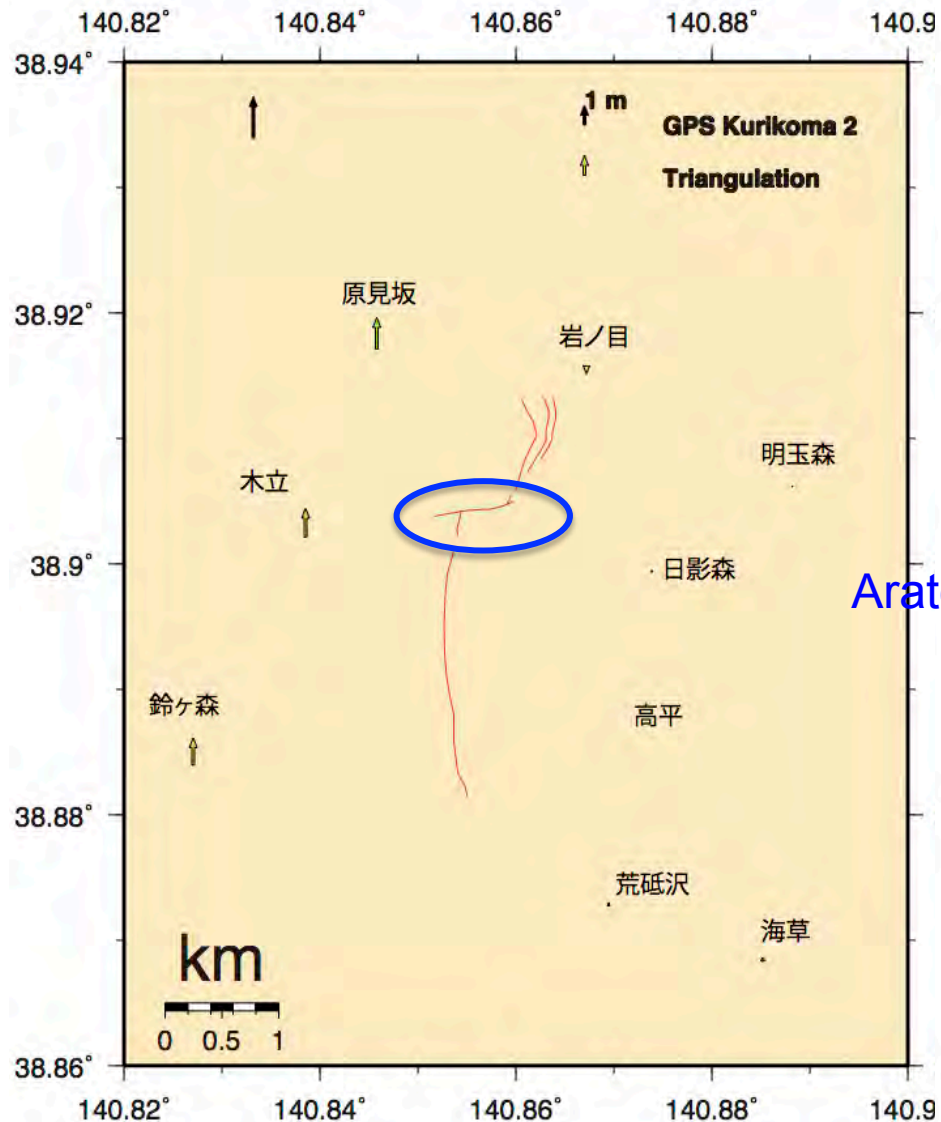


Takada et al. (2009)

Triangulation result around the site

Vertical (Post – Pre Eq.)

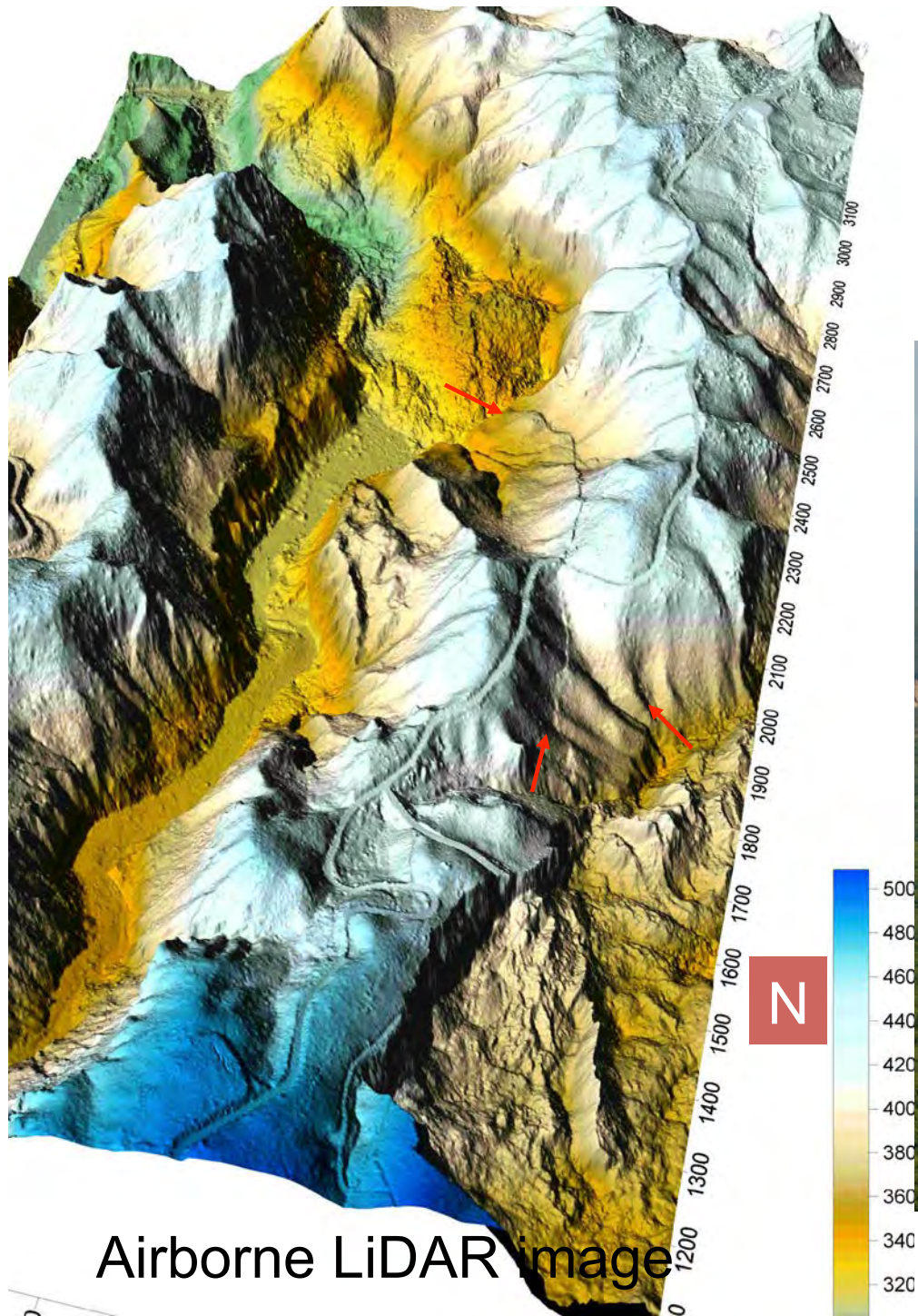
Horizontal (Post – Pre Eq.)



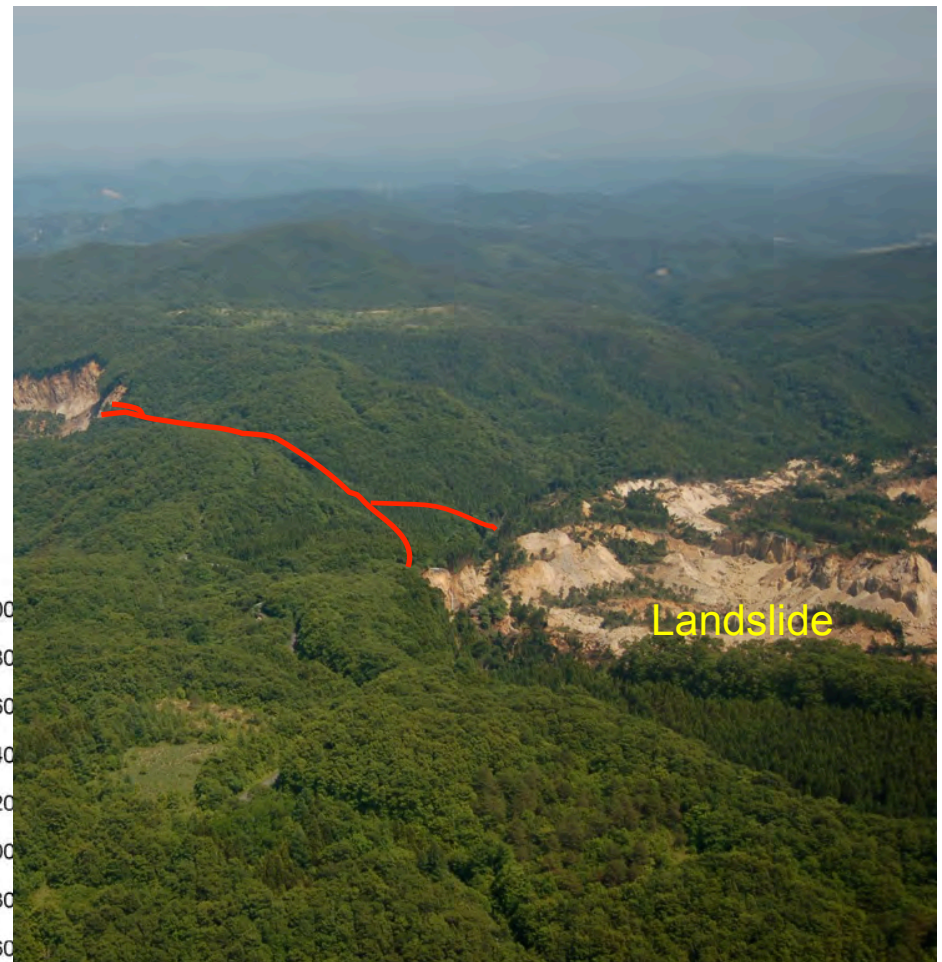
Aratozawa

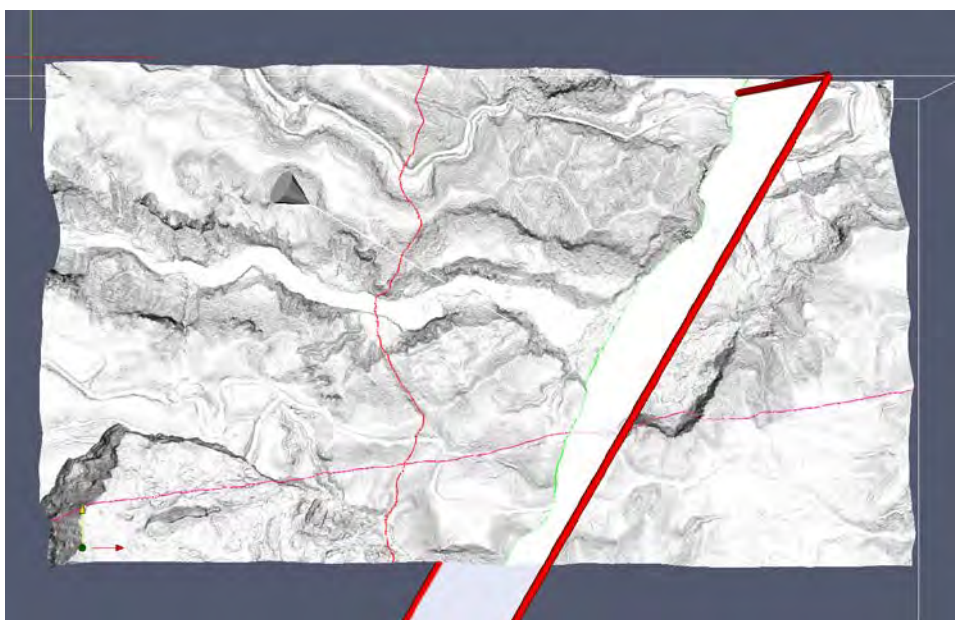
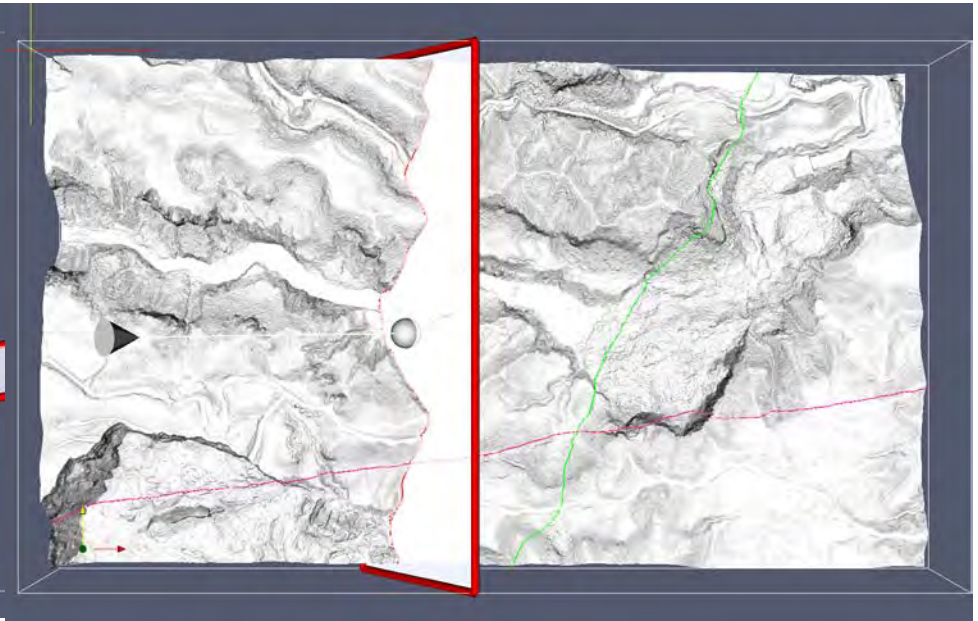
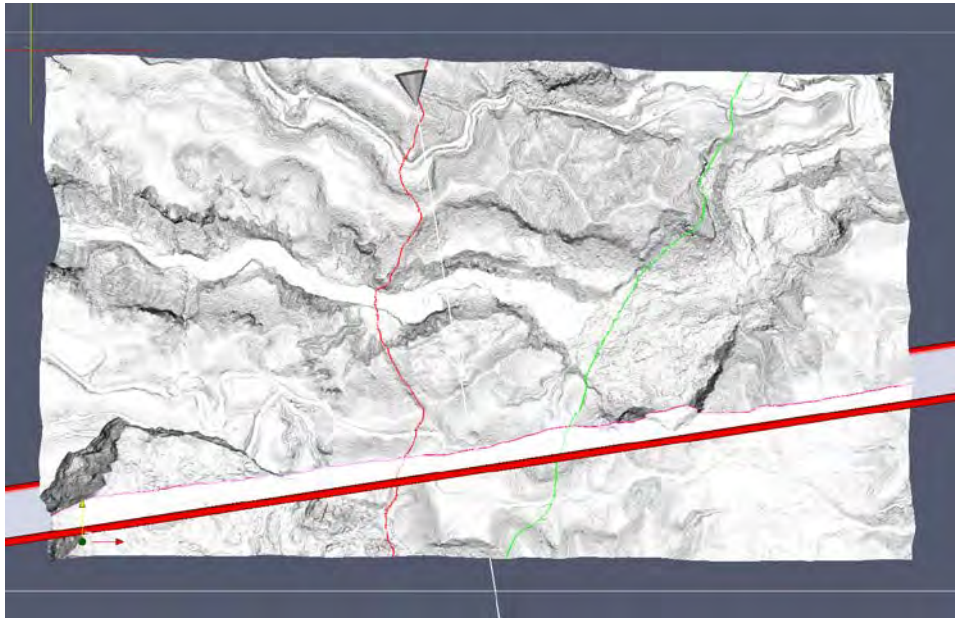
Awata (2009) Personal comm.

Consistent with reverse fault movement



Airborne LiDAR image





Combination of
2 thrust & 1 strike slip faults
explains surface trace

Yoshimi et al. (2008) @ AGU

1 m shortening



Yoshimi et al. (2008) @ AGU

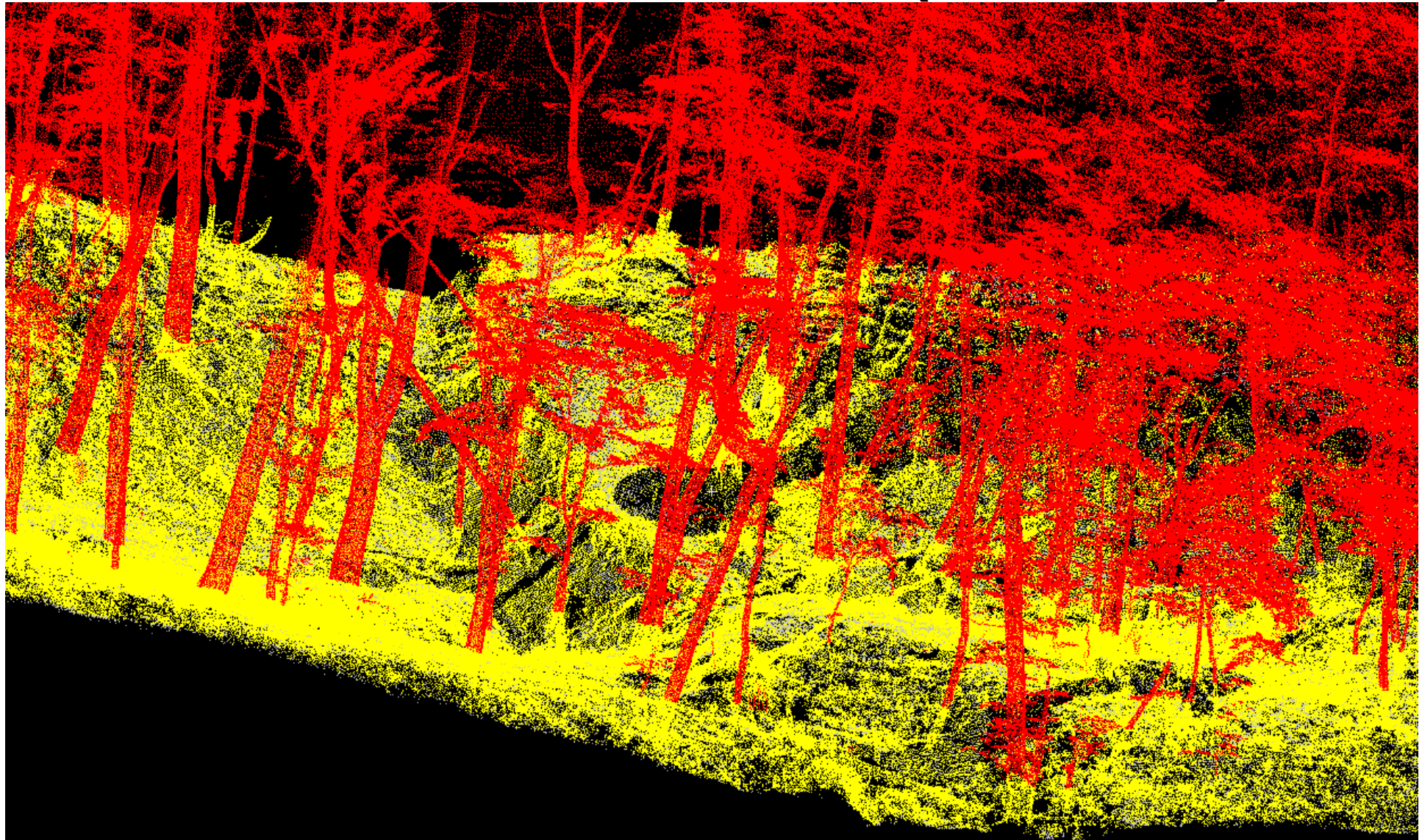
Large slip rupture



Large slip thrusting



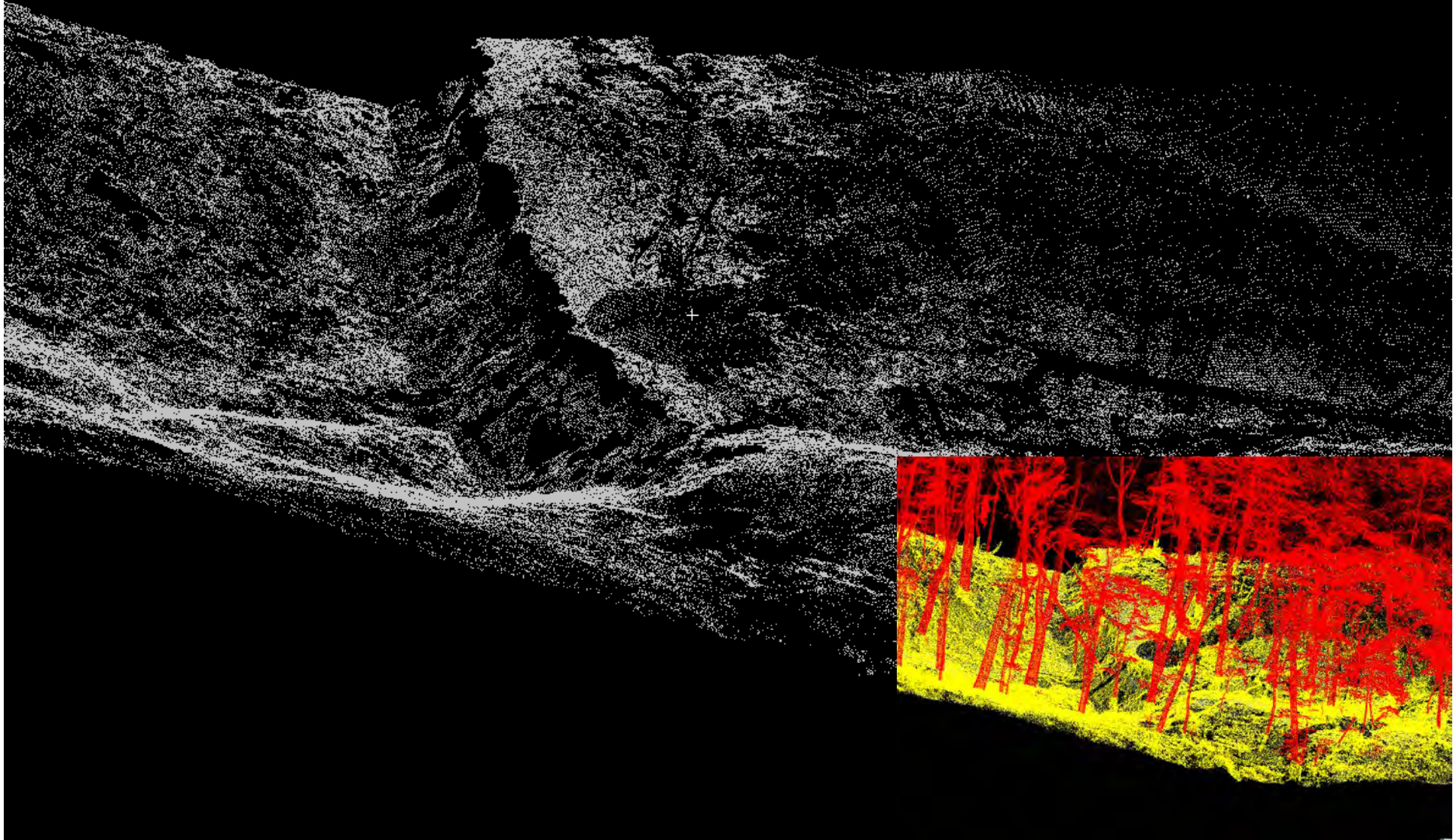
LiDAR Point Clouds (raw data)



Red : 1m above the ground surface
Yellow : vegetation

LiDAR Point Clouds (ground surface)

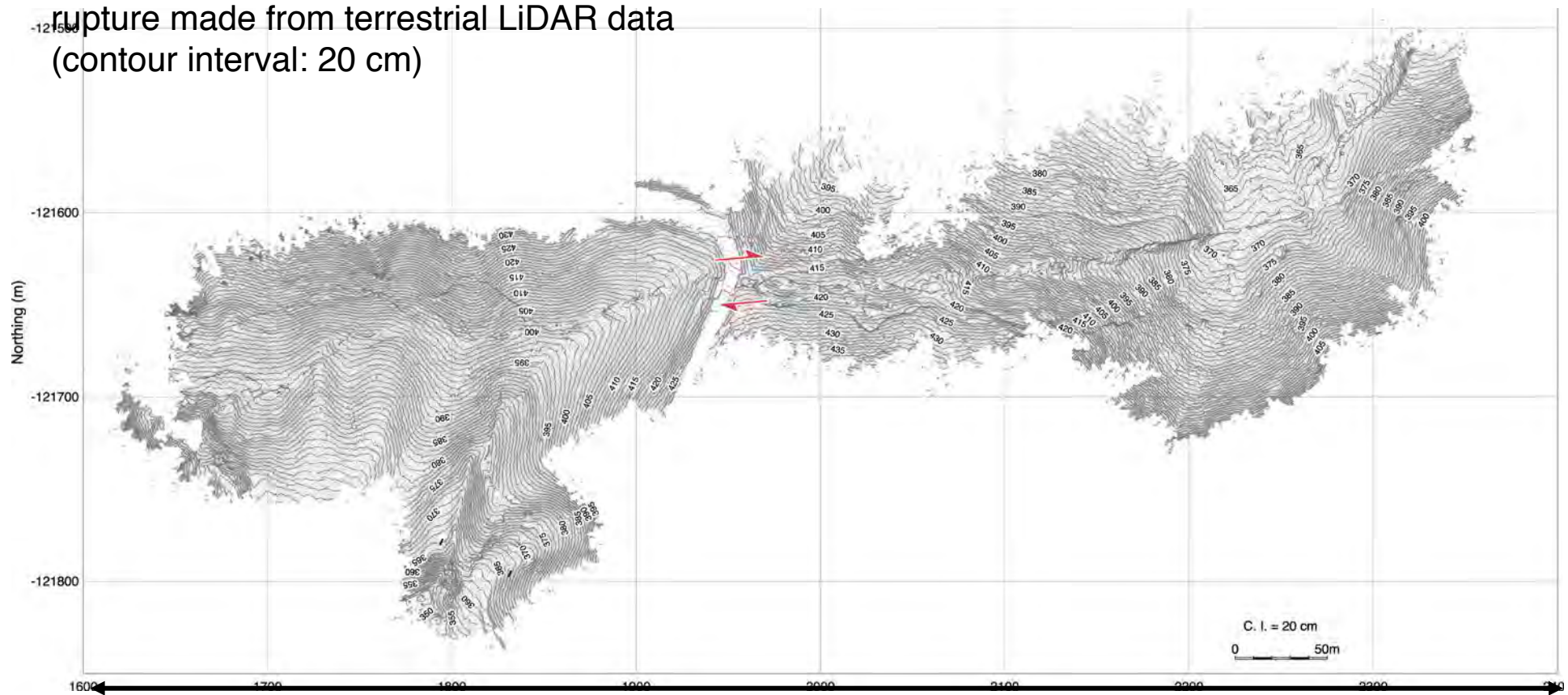
Point clouds after erasing vegetation offers ultra-fine view of the ground surface



Terrestrial LiDAR mapping

The LiDAR-derived ultra-high accuracy digital elevation models rendered overall topographic features associated with the ruptures

Topographic contour map along the surface rupture made from terrestrial LiDAR data (contour interval: 20 cm)



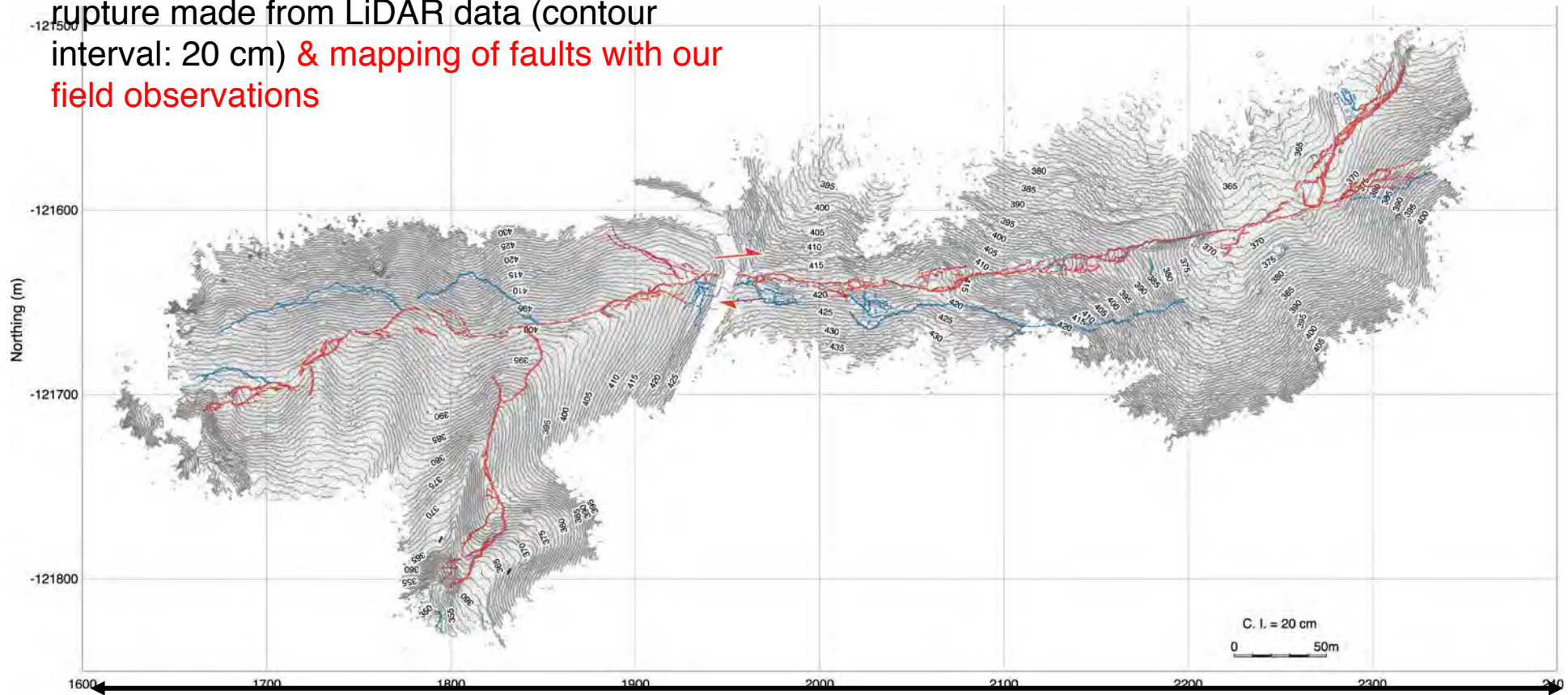
800 m

Maruyama, Toda, Yoshimi et al. (2009)

Terrestrial LiDAR mapping

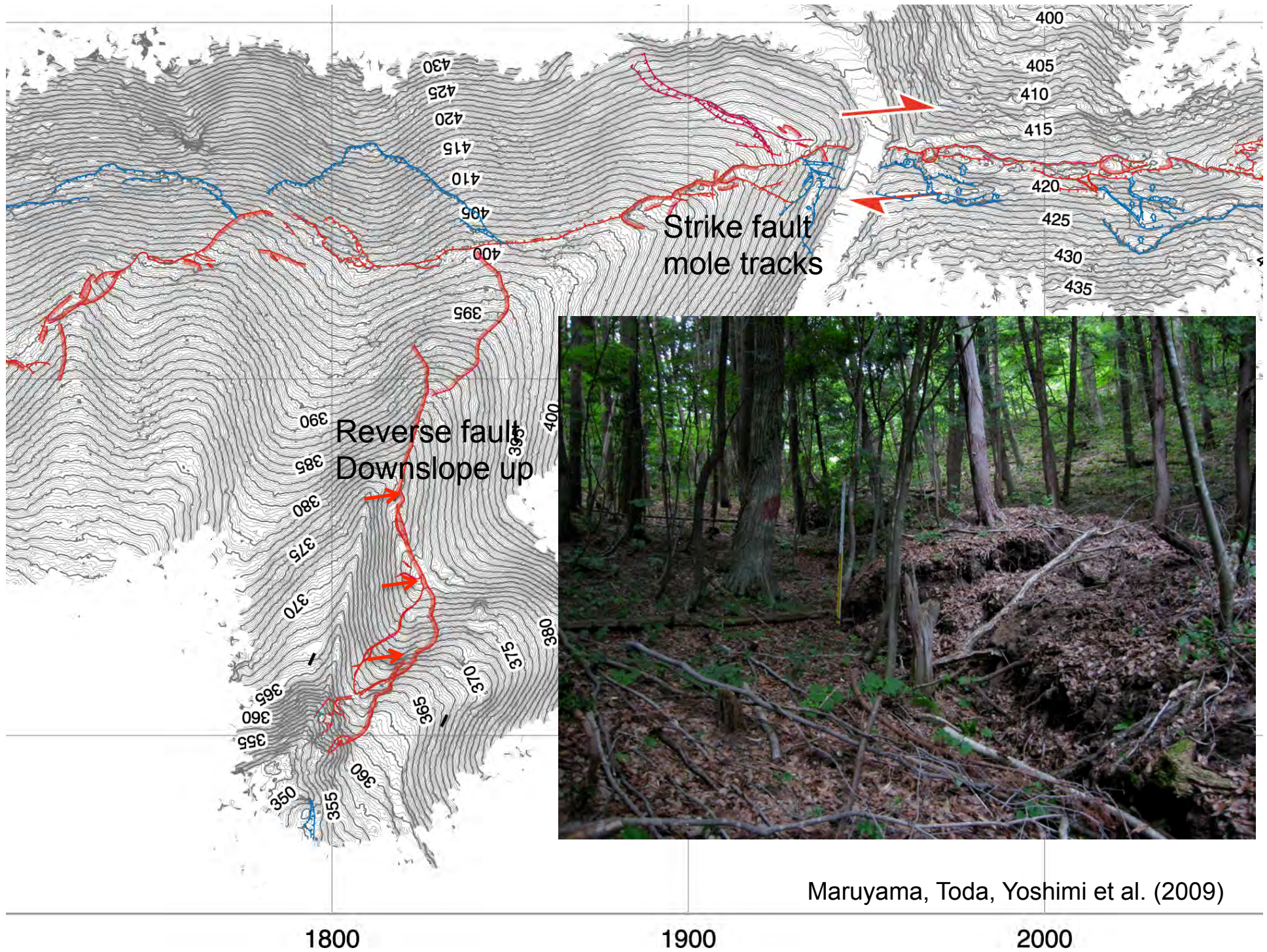
The LiDAR-derived ultra-high accuracy digital elevation models rendered overall topographic features associated with the ruptures

Topographic contour map along the surface rupture made from LiDAR data (contour interval: 20 cm) & mapping of faults with our field observations



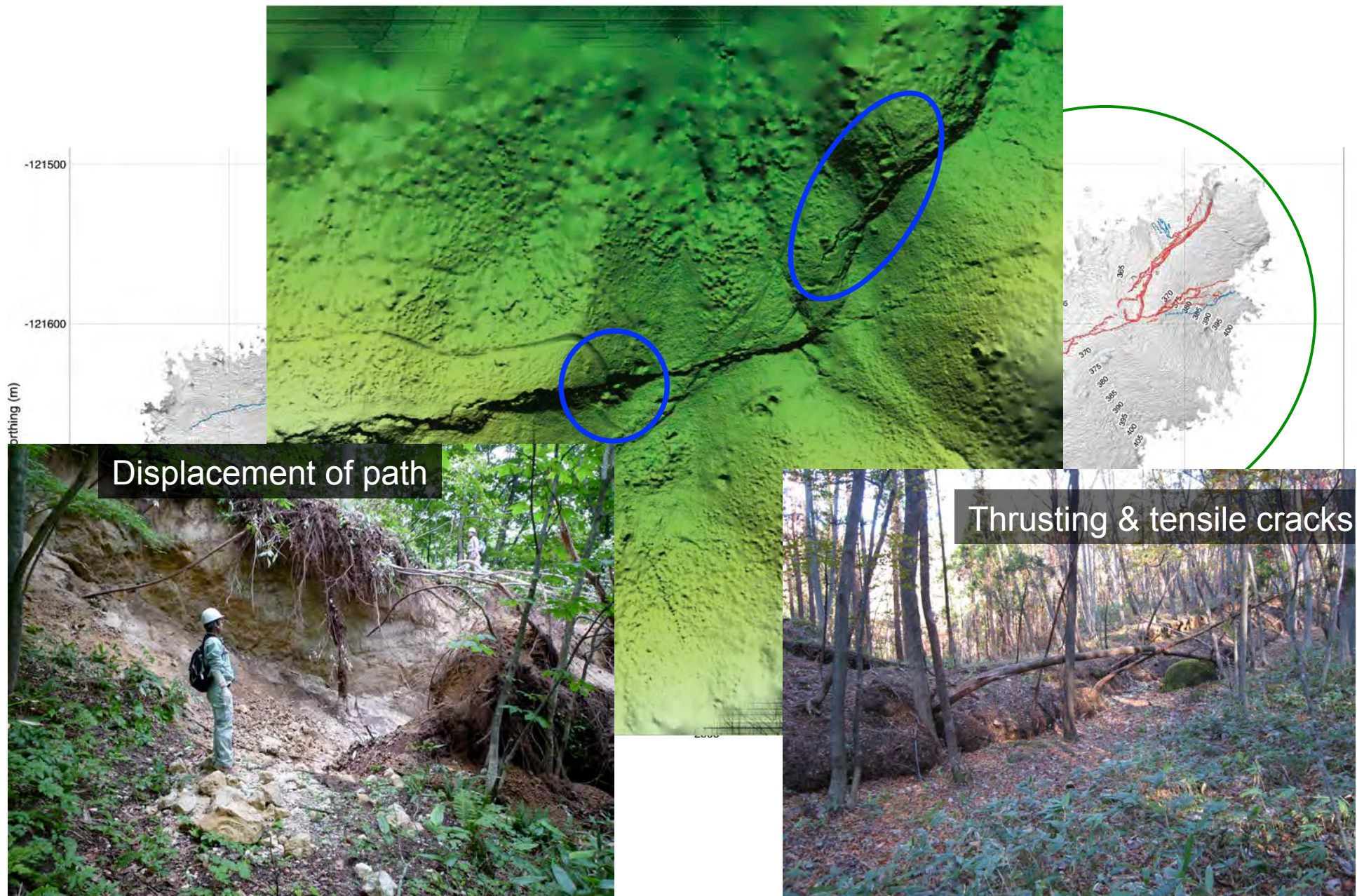
800 m

Maruyama, Toda, Yoshimi et al. (2009)



Maruyama, Toda, Yoshimi et al. (2009)

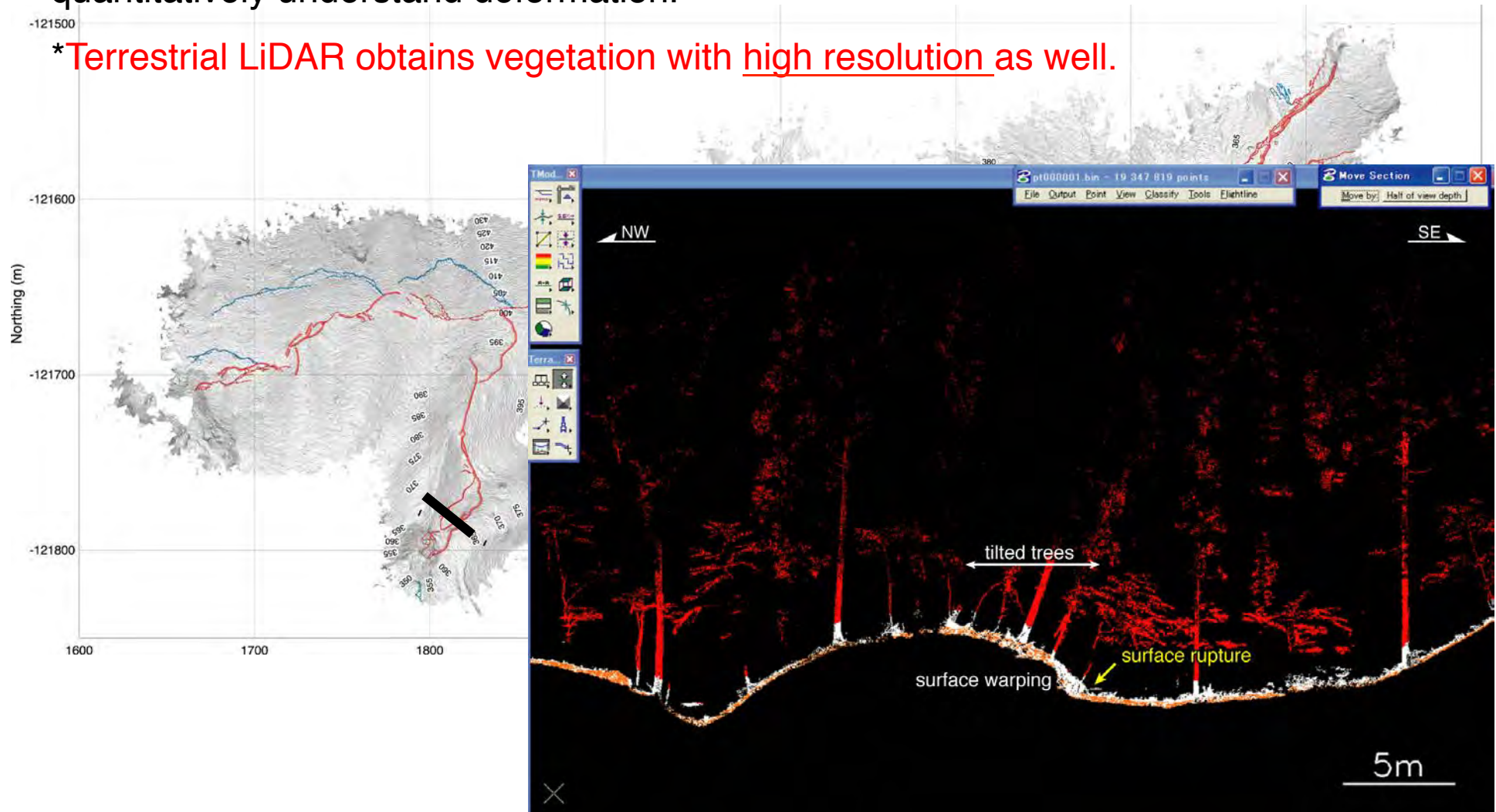
Terrestrial LiDAR mapping



Vivid imaging helped by trees and grass

We get ultra-fine topography data, but, need more information to quantitatively understand deformation.

*Terrestrial LiDAR obtains vegetation with high resolution as well.



Cypress tree tilting along the rupture

Tree tilting helps ground deformation recognition.

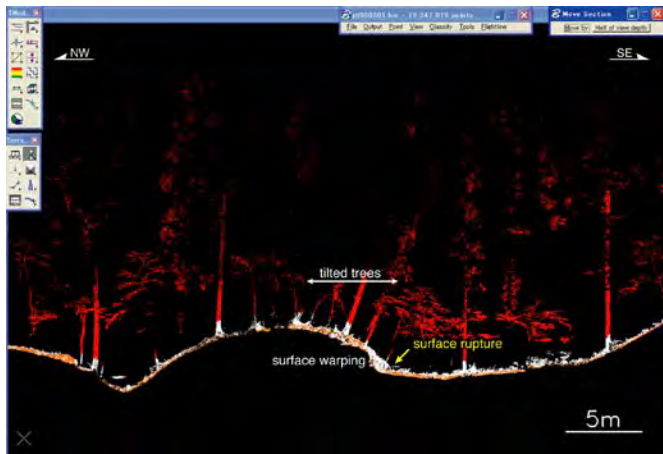
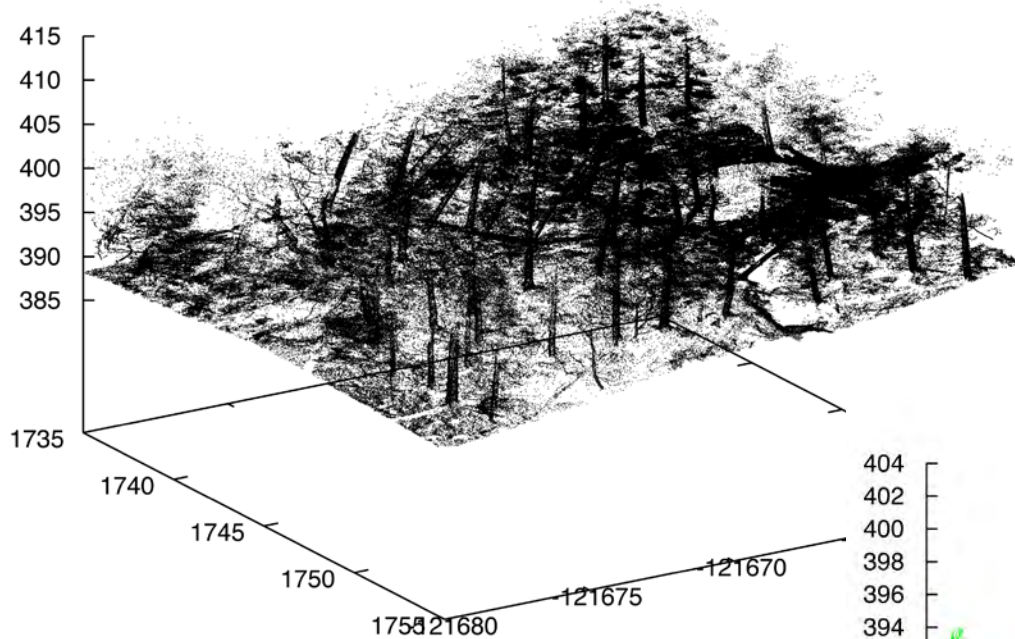


Photo by M.Yoshimi

Extraction of trees from point clouds

'./picked-points-demo.dat'

134,083,742 points

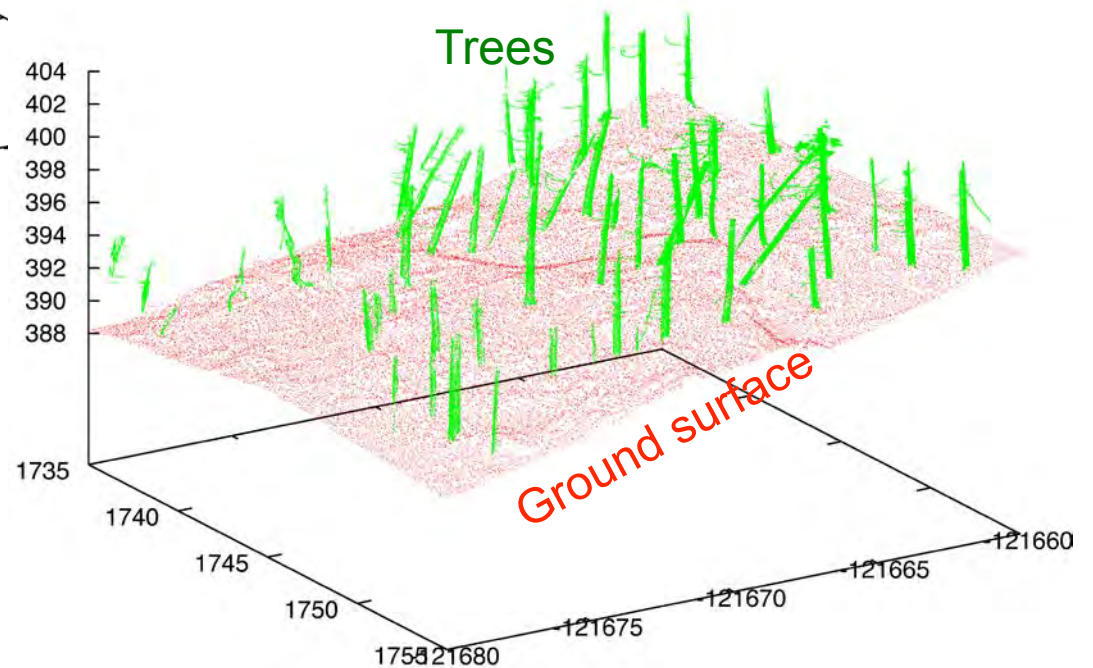


Raw point clouds
(figure: only small part)

Point classification

1st STEP Ground identification:
lowest and widest surface

2nd STEP: Tree grouping
group dense points with threshold
 $d < 2.5\text{cm}$, $h > 2\text{m}$, etc..

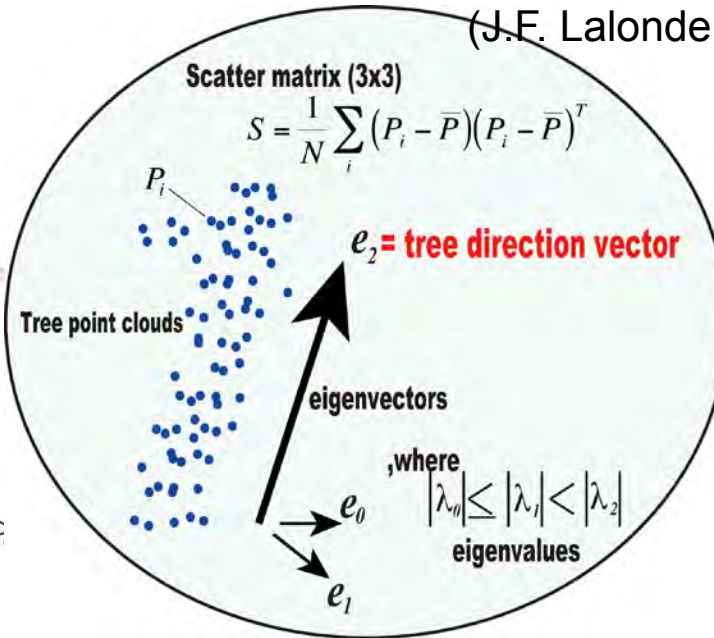
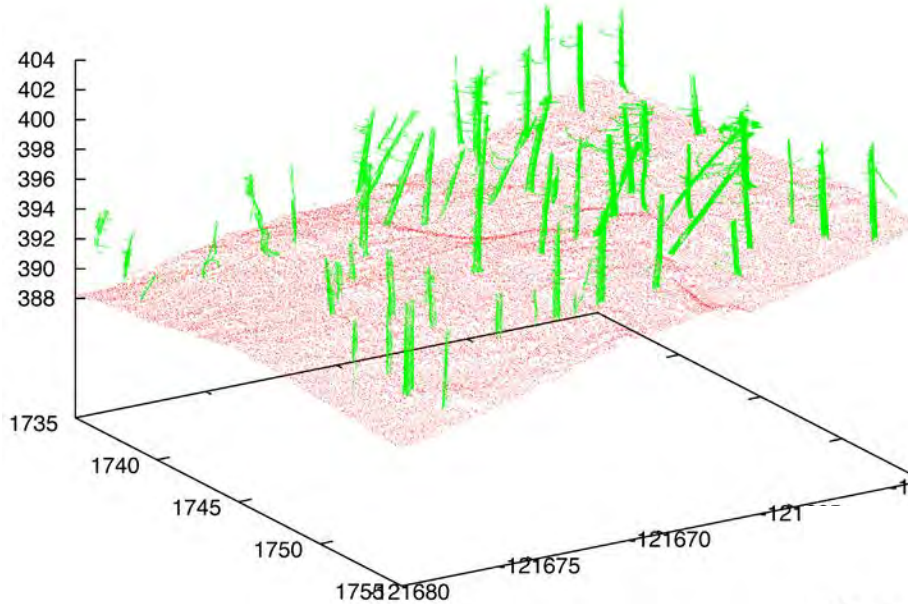


Yoshimi et al. (2009) ESC

17,194,745 points for >4000 trees

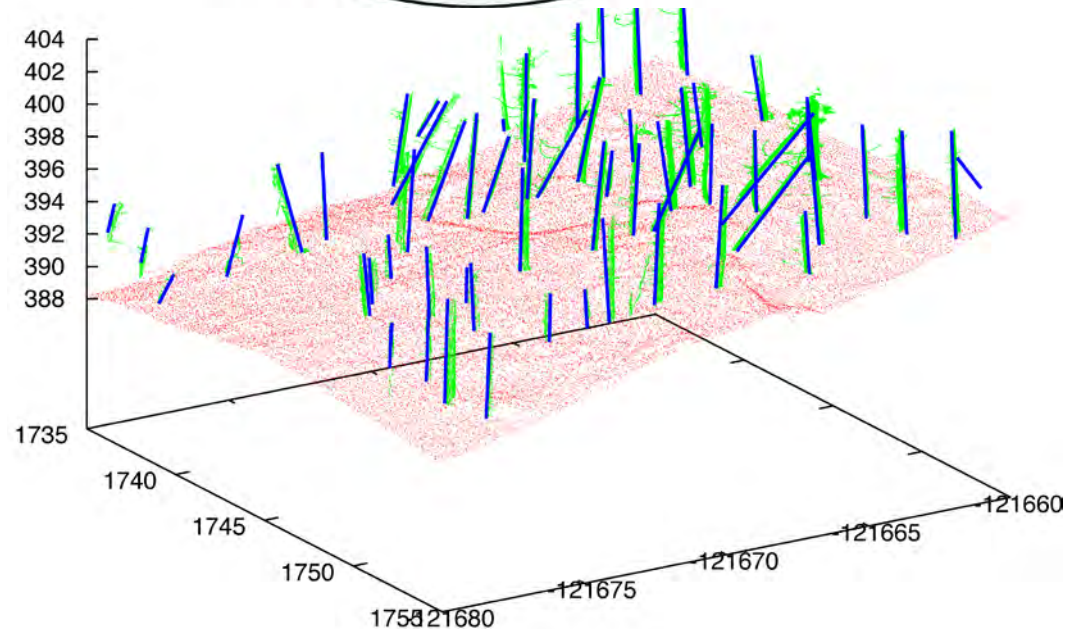
Tree direction vector from point clouds

(J.F. Lalonde, et al (2006))



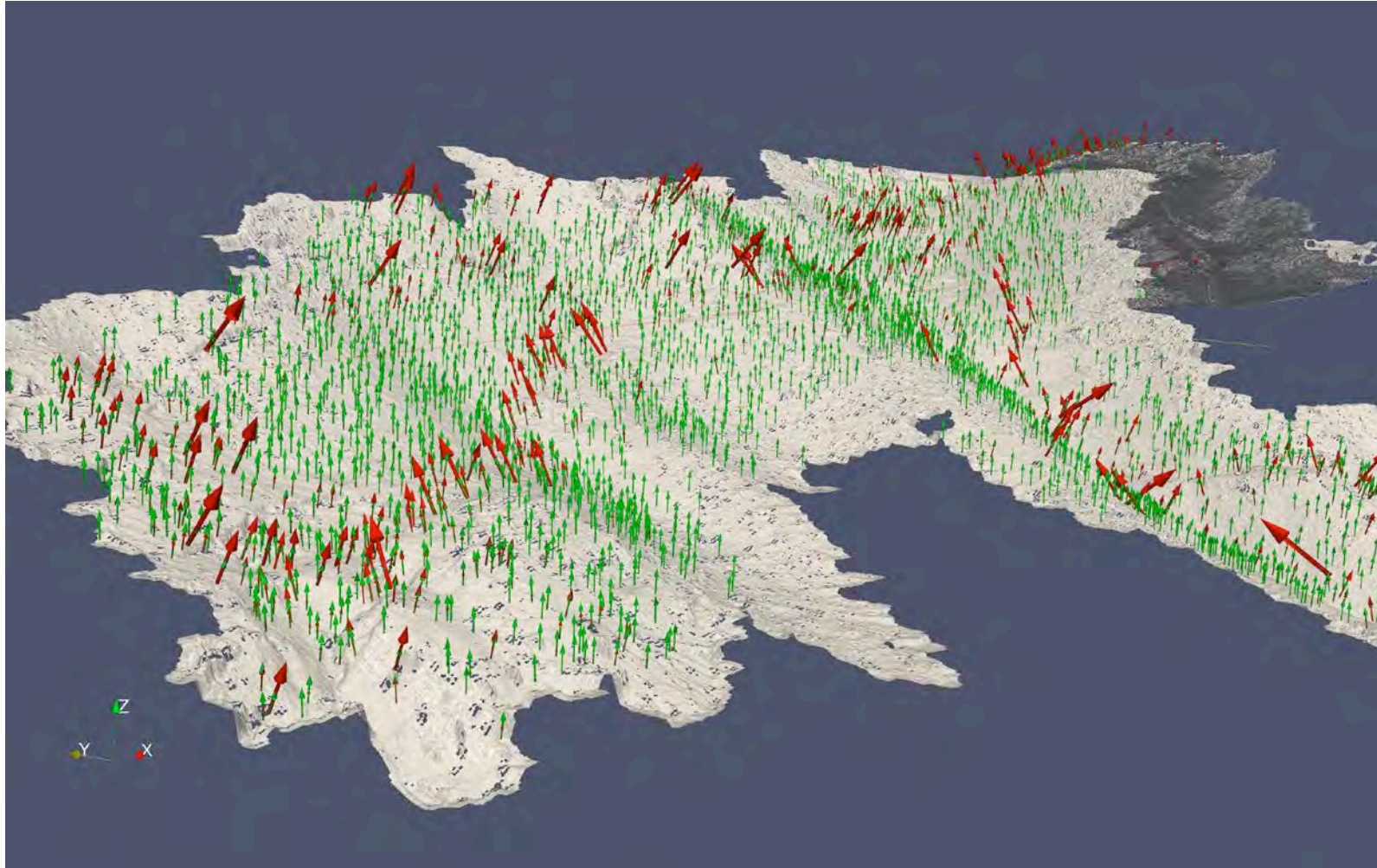
Principal component analysis of scatter matrix for each tree to obtain direction vector

Yoshimi et al. (2009) ESC



Tilted trees around surface rupture

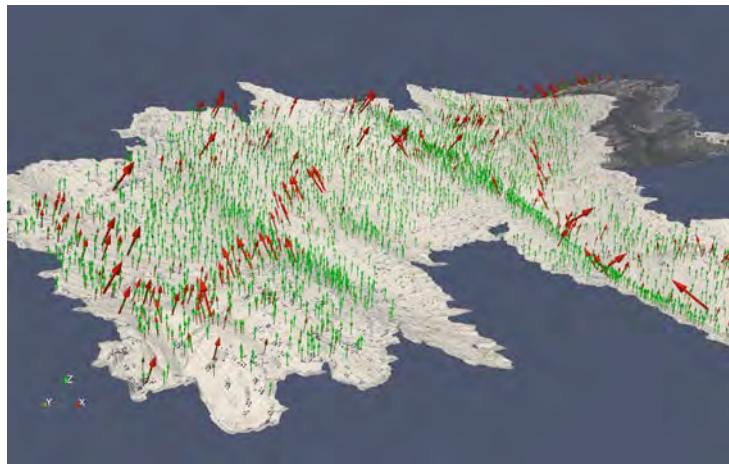
1. Tilted trees are concentrated around rupture.
2. Tilt directions show mechanical pattern associated with surface deformation.



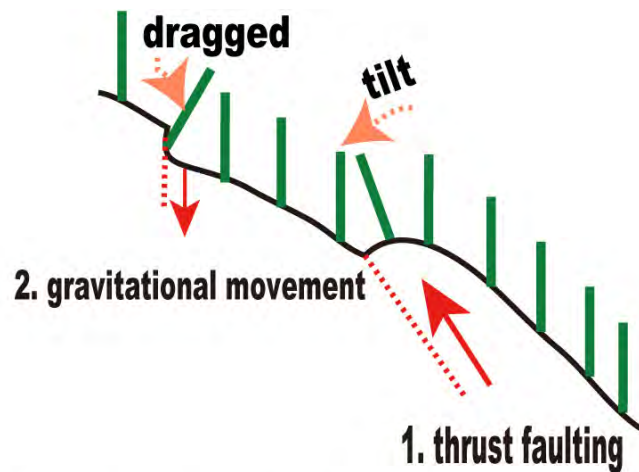
N=4768

Yoshimi et al. (2009) ESC

Tilt direction and angle distributions

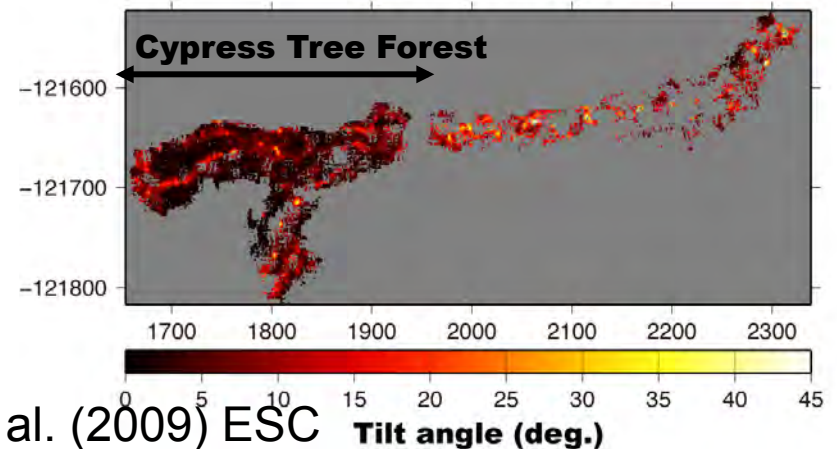
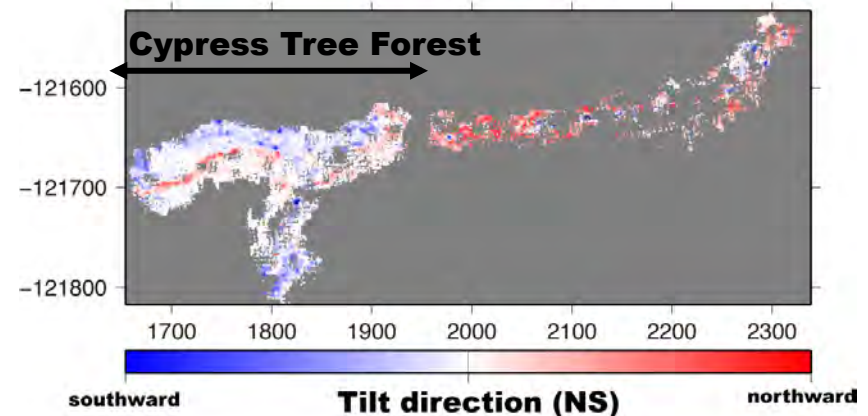
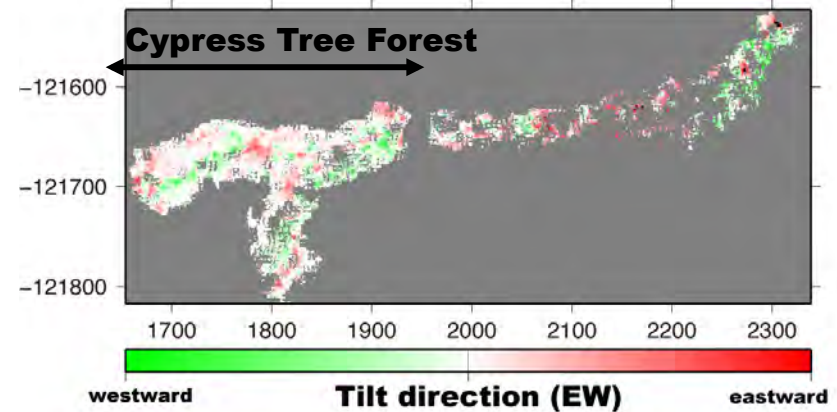


Deformation can be recognized from single image taken after rupturing if combined with tilting

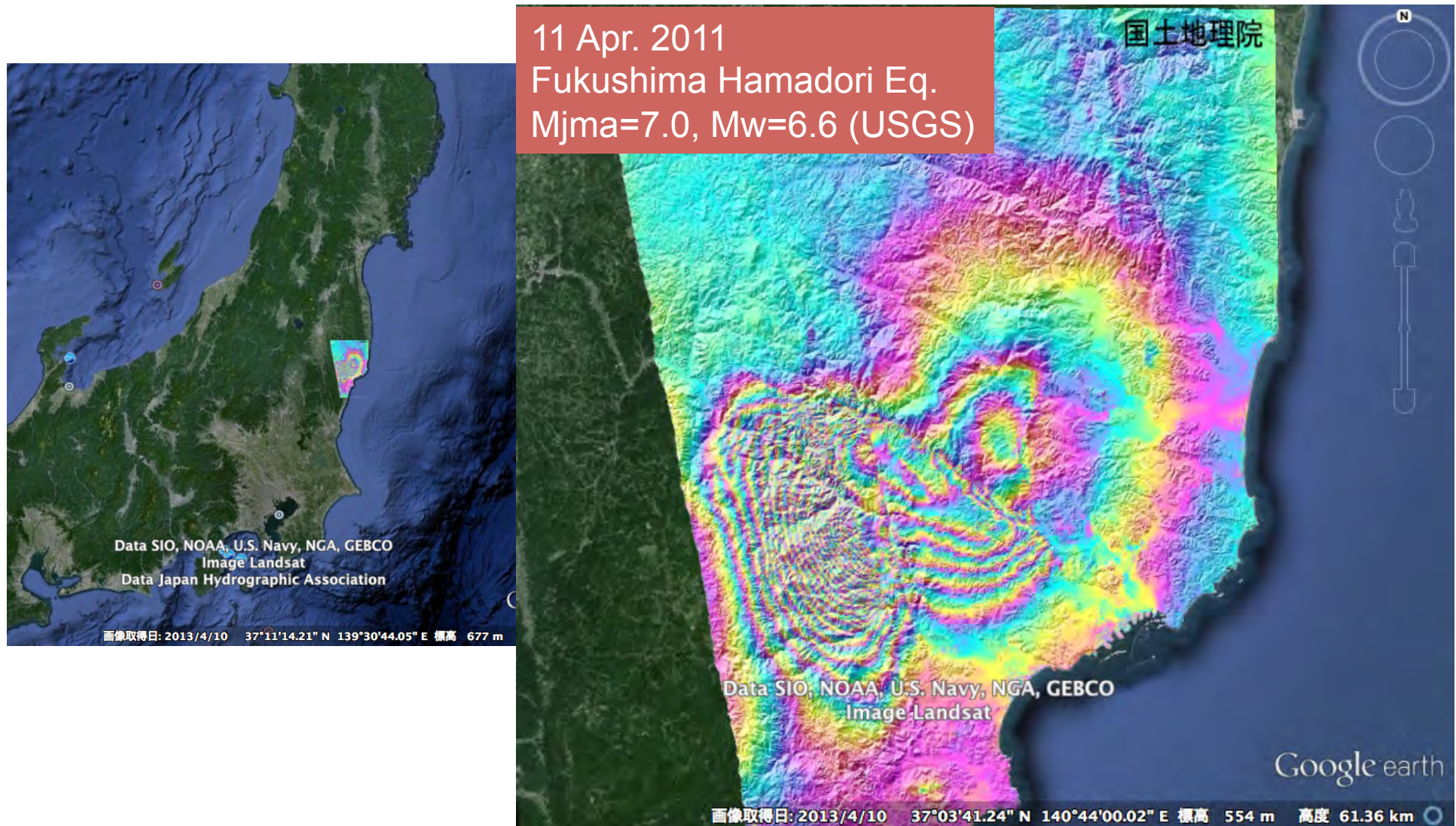


Relation of ruptures and trees tilting
(East part: cross section)

Yoshimi et al. (2009) ESC



2011 Fukushima Hamadori Eq.



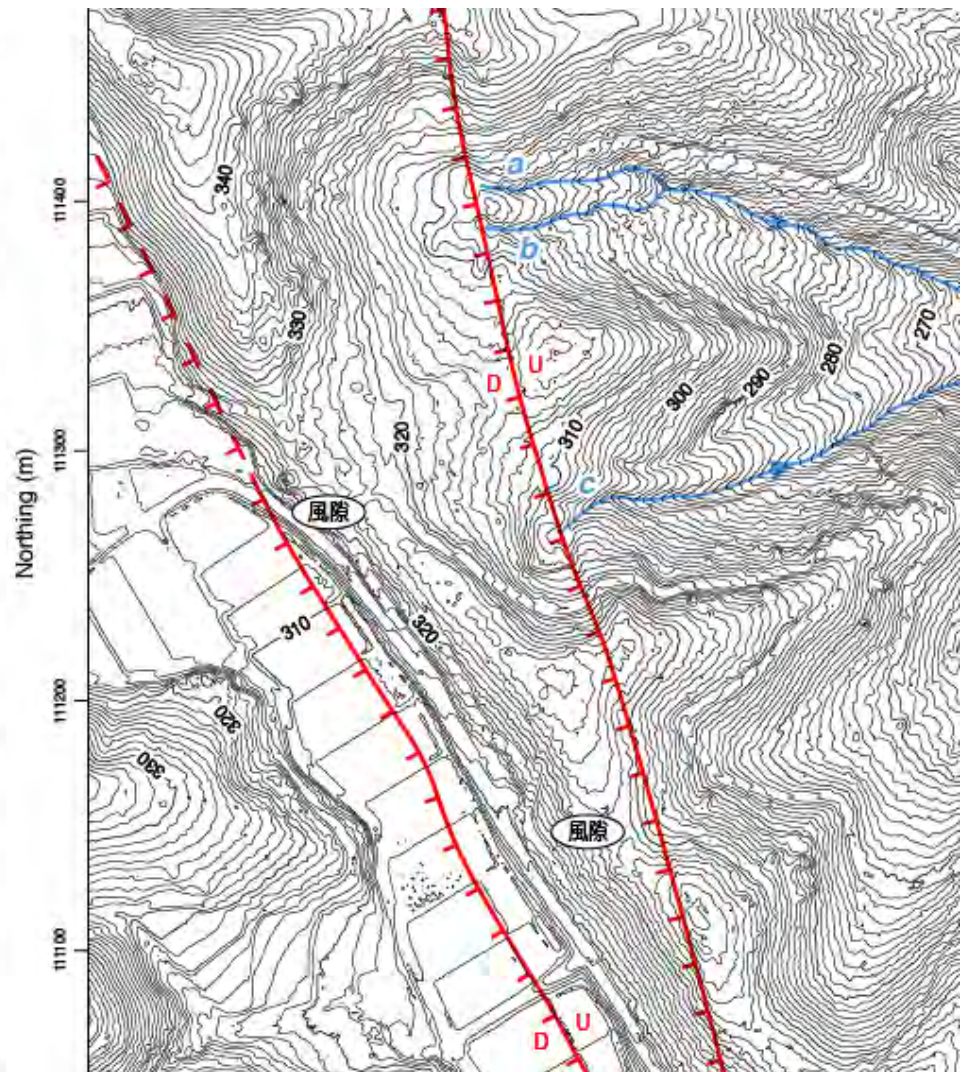
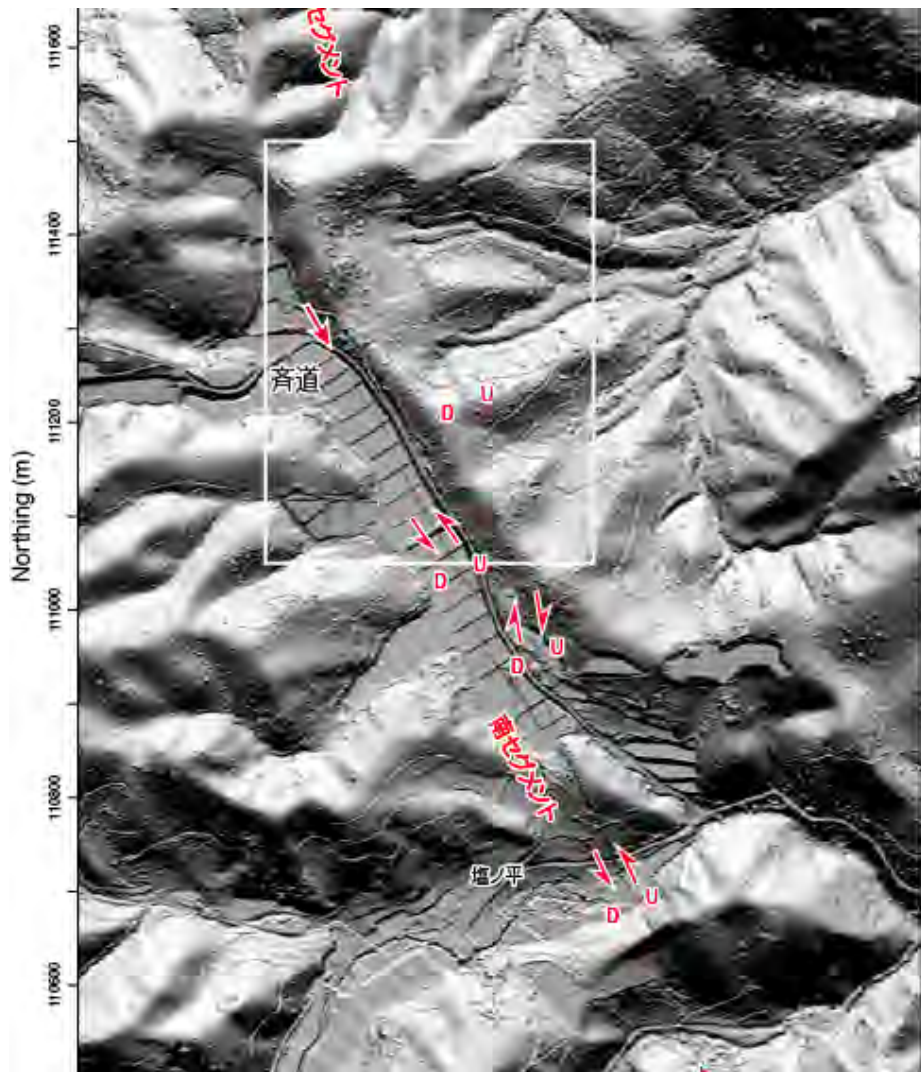
InSAR Image by GSI from ALOS

Idosawa Fault

Shiono Hira

InSAR Image by GSI from ALOS

Google earth

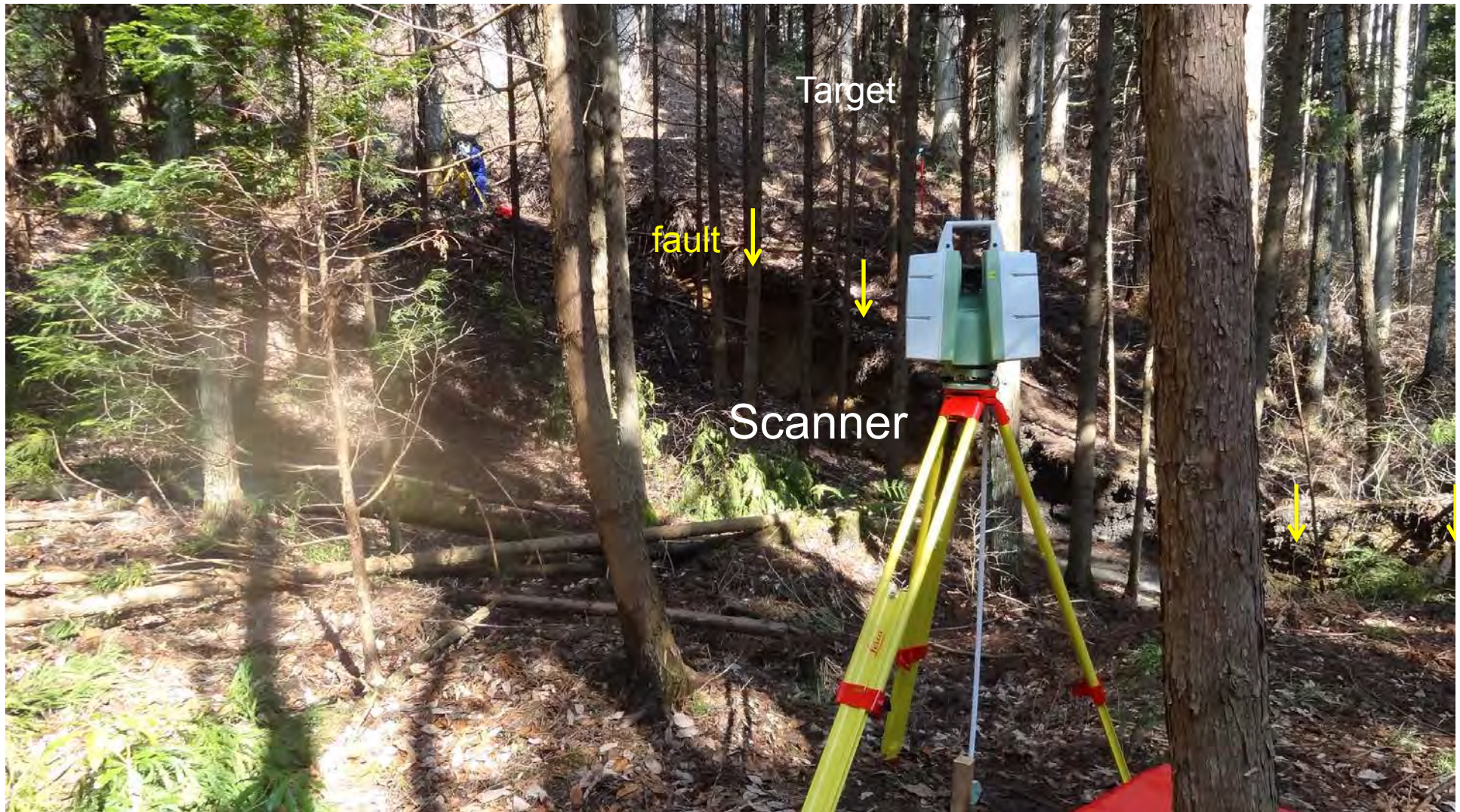


Surface rupture in the forest (Shionohira: Saido)



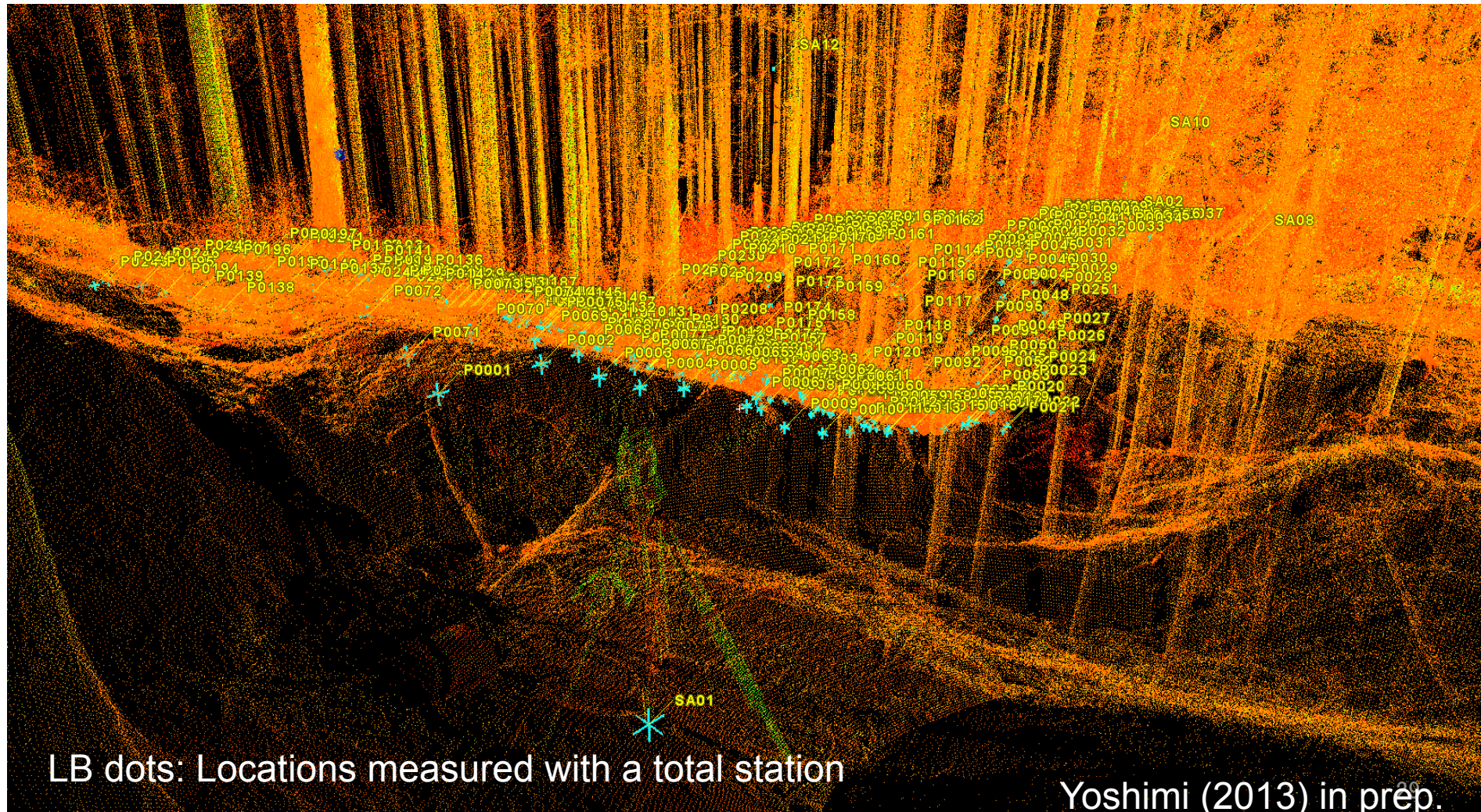
Yoshimi (2013) in prep.

Laser Scanning



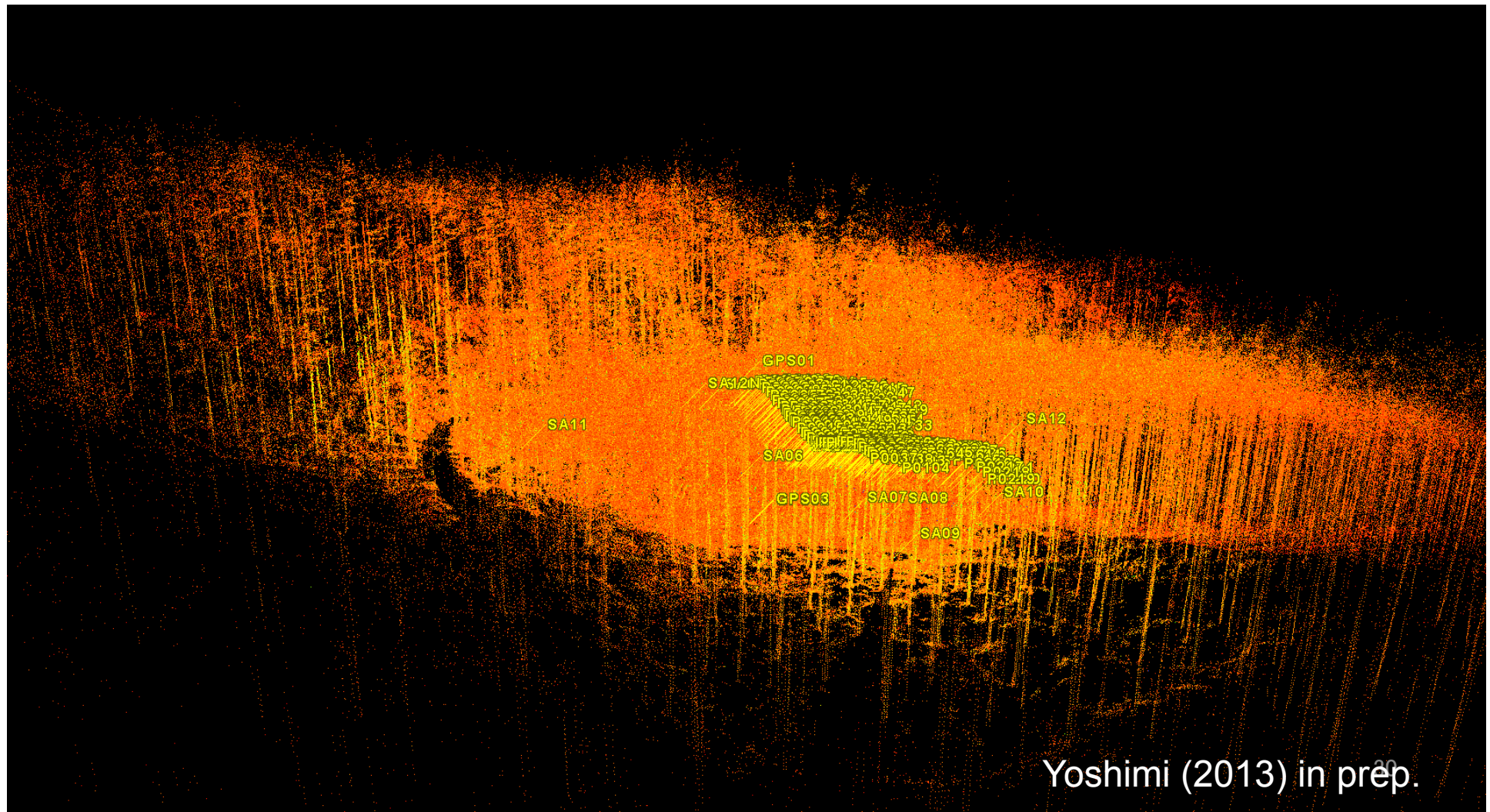
Yoshimi (2013) in prep.

Raw point clouds

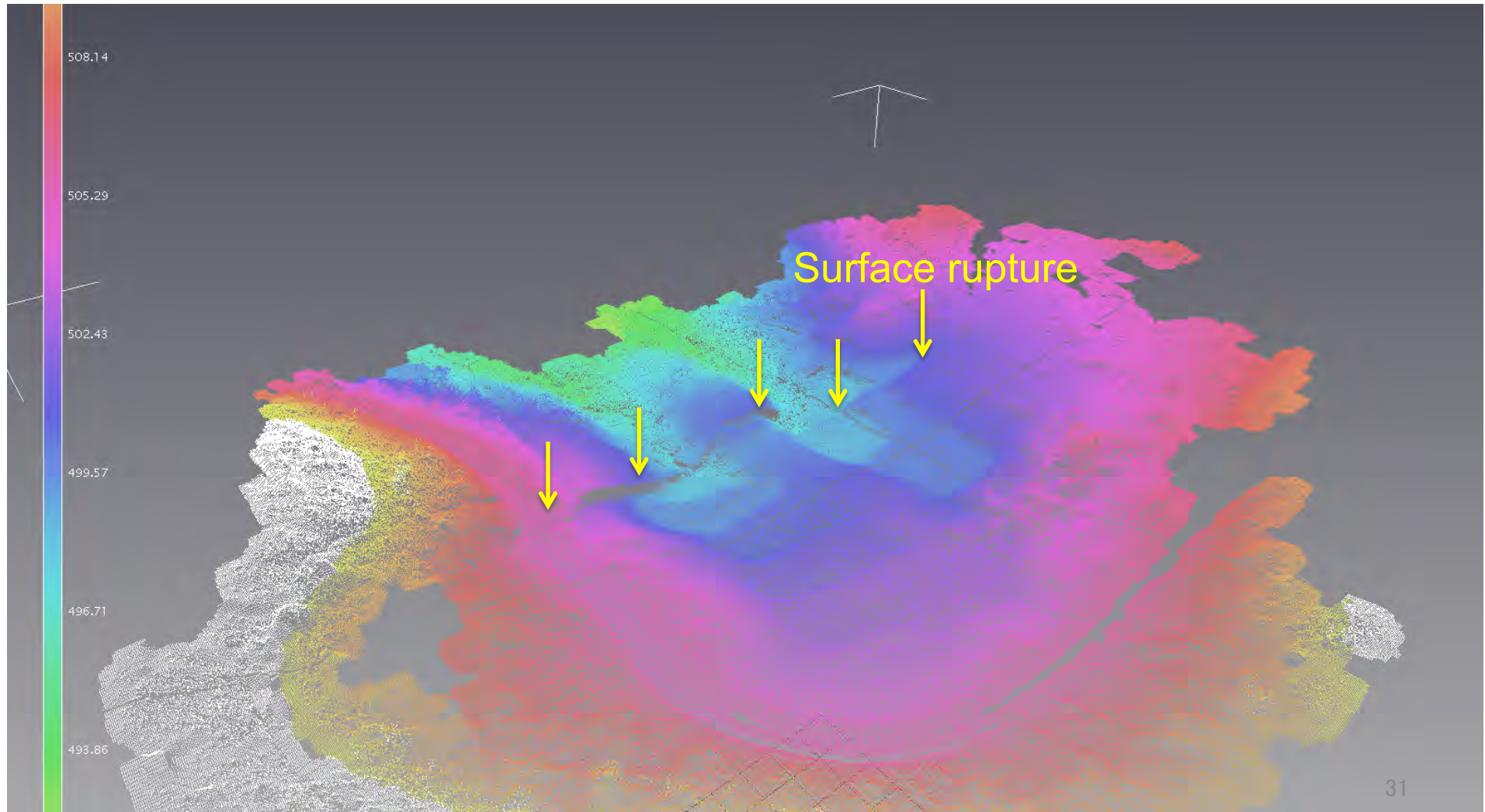


Point Clouds (30 million points)

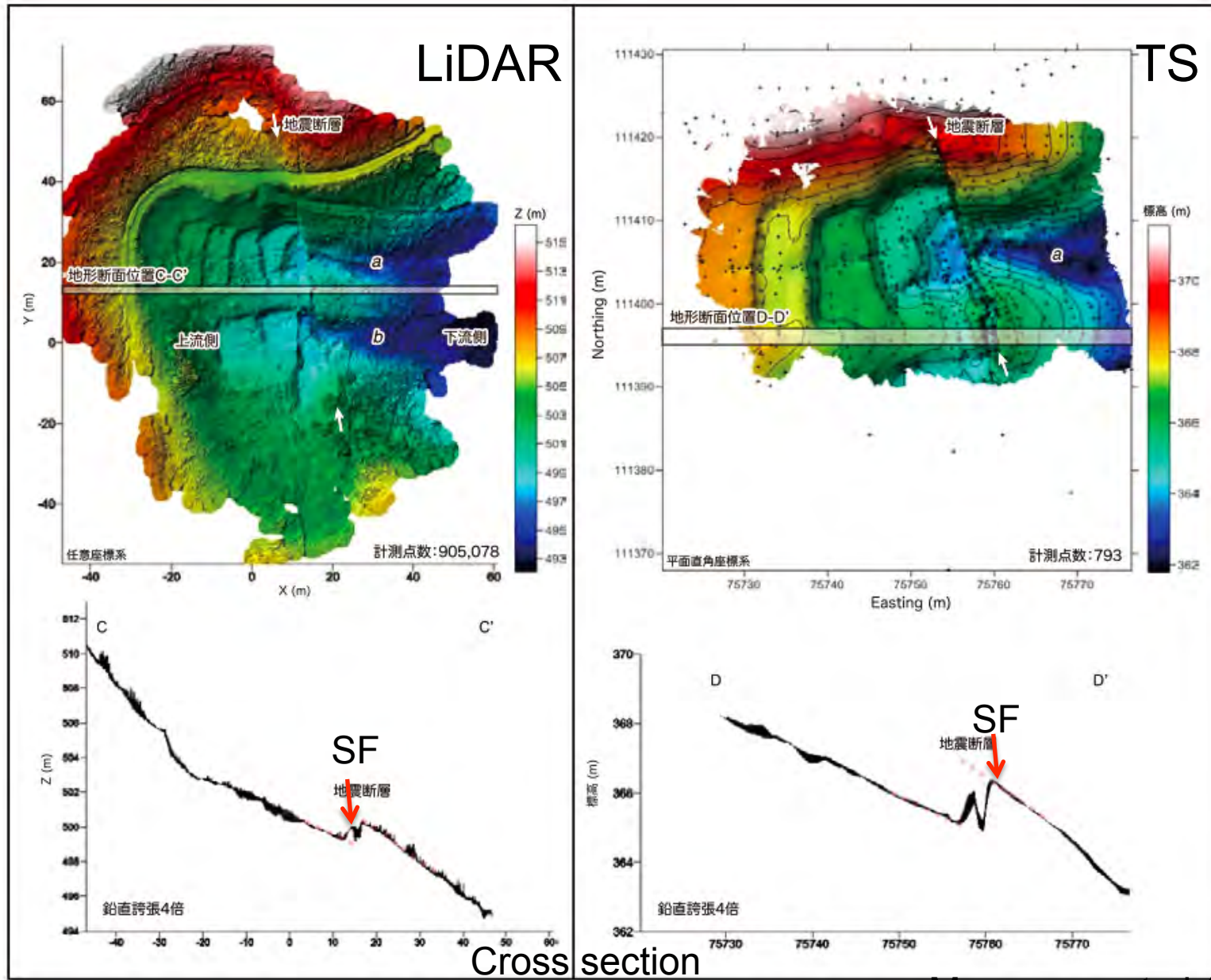
Scan from 13 locations



Extracted ground surface

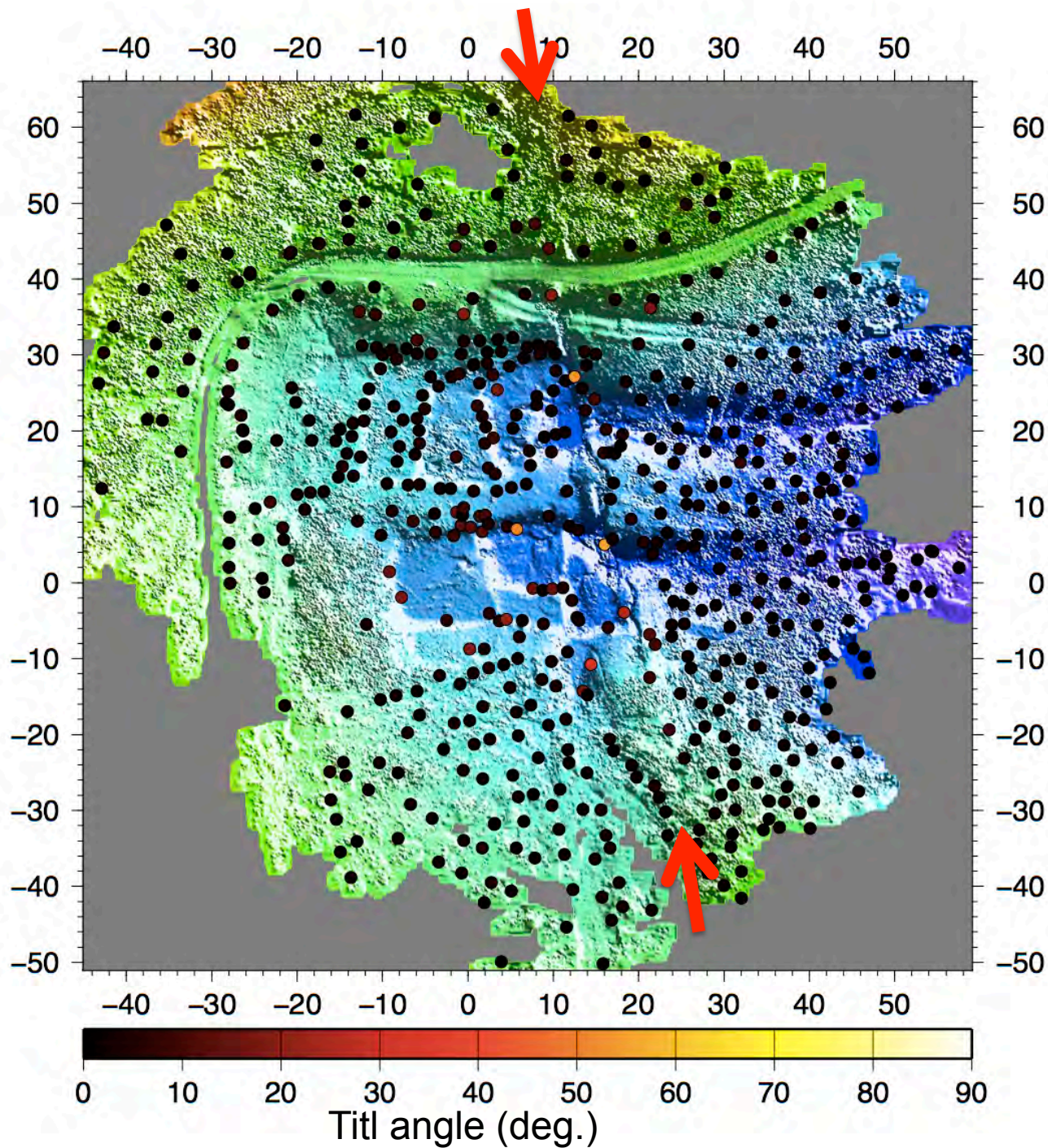


Yoshimi (2013) in prep.



Maruyama et al.(2012)

第 6 図 齊道地区周辺の詳細地形。左) 地上型レーザスキャナーを用いた計測結果。右) トータルステーションを用いた計測結果。右図の計測範囲は左図の北半分に対応。断面位置は、第 4 図左の断面 A-A' にほぼ一致₃₂。図中の a, b は第 4 図右に示した小河川 a, b に対応。いずれも 2012 年 2 月 23, 24 日に計測。



Tree tilt dist.

N=566

Tree tilting is not significant or concentrated around narrow area around the fault - Normal fault

Yoshimi (2013) in prep.



Reverse fault



Normal fault

Conclusions

- Terrestrial LiDAR was deployed for surface rupture of the 2008 Iwate-Miyagi Inland earthquake & 2011 Fukushima Hamadori Eq. to obtain fine topography.
- Terrestrial LiDAR is powerful tool for restoring vivid image of surface faulting.
- Trees can be tiltmeters on the ground when combined with LiDAR, which provide important information for structure design against deformation.